nature medicine

ARTICLES

https://doi.org/10.1038/s41591-020-0840-5

Check for updates

# Safety and feasibility of CRISPR-edited T cells in patients with refractory non-small-cell lung cancer

You Lu[1,14] ✉, Jianxin Xue[1,14], Tao Deng[2,14], Xiaojuan Zhou[1,14], Kun Yu[2,14], Lei Deng[3], Meijuan Huang[1], Xin Yi[4], Maozhi Liang[5], Yu Wang[6], Haige Shen[6], Ruizhan Tong[1], Wenbo Wang[7], Li Li[1], Jin Song[4], Jing Li[4], Xiaoxing Su[8], Zhenyu Ding[1], Youling Gong[1], Jiang Zhu[1], Yongsheng Wang[1,5], Bingwen Zou[1], Yan Zhang[1], Yanying Li[1], Lin Zhou[1], Yongmei Liu[1], Min Yu[1], Yuqi Wang[4], Xuanwei Zhang[1], Limei Yin[1], Xuefeng Xia[4], Yong Zeng[2], Qiao Zhou[9], Binwu Ying[10], Chong Chen[11], Yuquan Wei[11], Weimin Li[12] and Tony Mok[13]

**Clustered regularly interspaced short palindromic repeats (CRISPR)–Cas9 editing of immune checkpoint genes could improve the efficacy of T cell therapy, but the first necessary undertaking is to understand the safety and feasibility. Here, we report results from a first-in-human phase I clinical trial of CRISPR–Cas9 *PD-1*-edited T cells in patients with advanced non-small-cell lung cancer (ClinicalTrials.gov NCT02793856). Primary endpoints were safety and feasibility, and the secondary endpoint was efficacy. The exploratory objectives included tracking of edited T cells. All prespecified endpoints were met. *PD-1*-edited T cells were manufactured ex vivo by cotransfection using electroporation of Cas9 and single guide RNA plasmids. A total of 22 patients were enrolled; 17 had sufficient edited T cells for infusion, and 12 were able to receive treatment. All treatment-related adverse events were grade 1/2. Edited T cells were detectable in peripheral blood after infusion. The median progression-free survival was 7.7 weeks (95% confidence interval, 6.9 to 8.5 weeks) and median overall survival was 42.6 weeks (95% confidence interval, 10.3–74.9 weeks). The median mutation frequency of off-target events was 0.05% (range, 0–0.25%) at 18 candidate sites by next generation sequencing. We conclude that clinical application of CRISPR–Cas9 gene-edited T cells is generally safe and feasible. Future trials should use superior gene editing approaches to improve therapeutic efficacy.**

CRISPR–Cas9 technology offers a convenient, flexible and precise method for genome editing[1,2]. Cas9, typically *Streptococcus pyogenes* Cas9 (SpCas9)[3], recognizes a protospacer-adjacent motif (PAM) upstream or downstream of the target sequence by using a guide RNA and induces double-stranded breaks in the target DNA. The clinical application of CRISPR editing has been unclear, as CRISPR–Cas9 could cause genotoxicity including off-target genome cleavage sites, chromosomal translocations or other complex changes, which may lead to unpredictable consequences[4]. Recent pilot clinical trials using CRISPR-edited stem cells and multigene-edited T cells in the treatment of HIV/AIDS and cancer, including multiple myeloma and sarcoma, support the safety and feasibility of CRISPR–Cas9 technology in the clinic[5,6]. Anti-PD-1 checkpoint inhibitors such as pembrolizumab have become the standard first-line therapy for advanced non-small-cell lung cancer (NSCLC) with PD-L1 expression[7,8]. Some patients may attain 5-yr survival rates of 15.5–23% with single-agent pembrolizumab[9]. We hypothesized that disruption of the *PD-1* gene in T cells followed by ex vivo reinfusion of the gene-edited cells could be therapeutic. While specific data on lung cancer are lacking, preclinical data have shown that editing of *PD-1* in tumor-infiltrating lymphocytes by zinc finger nuclease improves T cell cytotoxicity in melanoma, and that T cells edited via CRISPR–Cas9 show enhanced anti-tumor responses against gastric cancer[10,11]. As lung cancer is the most prevalent and fatal malignancy in China and worldwide[12,13], we chose to focus on treatment of this disease.

Being conscious of the potential ethical implications and risk of off-target mutations, we enrolled patients with NSCLC who failed multiple lines of therapy in a dose-escalating phase I clinical trial. The primary objectives were to demonstrate the feasibility of gene-edited T cell therapy and to evaluate safety. The gene-edited cells were expanded ex vivo and re-infused as therapeutic T cells. To monitor the risk of off-target mutations, we performed

[1]Department of Thoracic Oncology, Cancer Center and State Key Laboratory of Biotherapy, West China Hospital, Sichuan University, Chengdu, China. [2]Chengdu MedGenCell, Co., Ltd, Chengdu, China. [3]Jacobi Medical Center, NYC Health Hospitals, Albert Einstein College of Medicine, New York, NY, USA. [4]Geneplus-Beijing Institute, Beijing, China. [5]Center of GCP, West China Hospital, Sichuan University, Chengdu, China. [6]ZenRhyme Consulting Service, Ltd, Shanghai, China. [7]National Research Center for Translational Medicine, Ruijin Hospital Affiliated to Shanghai Jiao Tong University School of Medicine, Shanghai, China. [8]Berry Oncology Co. Ltd, Fujian, China. [9]Department of Pathology, West China Hospital, Sichuan University, Chengdu, China. [10]Department of Laboratory Medicine, West China Hospital, Sichuan University, Chengdu, China. [11]State Key Laboratory of Biotherapy and Collaborative Innovation Center for Biotherapy, West China Hospital, Sichuan University, Chengdu, China. [12]Department of Respiratory and Critical Care Medicine and Frontier Science Center of Disease Molecular Network, West China Hospital, Sichuan University, Chengdu, China. [13]State Key Laboratory of Translational Oncology, Department of Clinical Oncology, Chinese University of Hong Kong, Hong Kong, China. [14]These authors contributed equally: You Lu, Jianxin Xue, Tao Deng, Xiaojuan Zhou, Kun Yu. ✉e-mail: radyoulu@hotmail.com

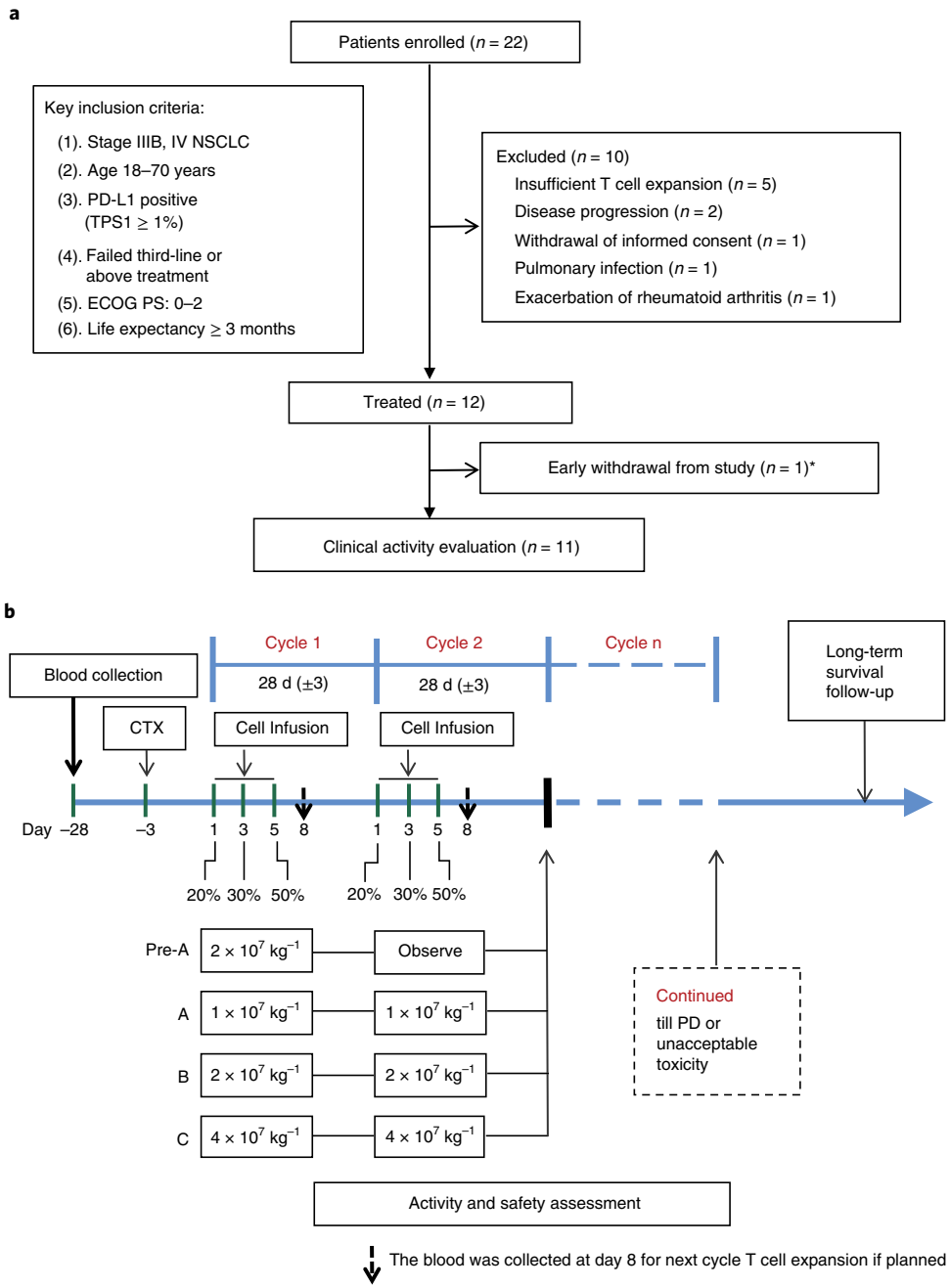


**Fig. 1 | Schematic showing patient flow and study design, including patient enrollment, planned dose cohorts, interventions, follow-up and outcome assessments. a**, A Consolidated Standards of Reporting Trials (CONSORT) diagram showing patient flow through the main stages in the phase I dose-escalation trial. **b**, Study design. The *PD-1* gene-edited T cells were infused every 28 d (cycle) as three infusions, the first containing 20% of the indicated total cell number; the second, 30%; and the third, 50%. PD, progressive disease; TPS, tumor proportion score; ECOG PS, Eastern Cooperative Oncology Group performance status; CTX, cyclophosphamide (20 mg kg$^{-1}$). Asterisks show that the patient could not be evaluated for treatment efficacy owing to early withdrawal from the trial due to a bacterial infection that caused exacerbation of pulmonary disease after the first treatment cycle.

whole-genome sequencing (WGS) and next generation sequencing (NGS) on genomic DNA isolated from edited T cells before infusion. In addition, we evaluated in vivo tracking of edited T cells, peripheral T cell receptor (TCR) clone diversity and unique TCR clones in peripheral blood mononuclear cells (PBMCs) during and following therapy.

## Results

**Patients and treatment.** A total of 22 patients were enrolled from 26 August 2016 to 21 March 2018 (Fig. 1). Five patients did not ultimately receive infusions because of insufficient expansion of T cells. We succeeded in manufacturing sufficient and high-viability (>90%) edited T cells (success rate, 77.3%, 17 of 22) for the remaining 17 patients. Five of 17 patients were excluded before T cell infusion for disease progression (two), consent withdrawal (one), pulmonary infection (one) and exacerbation of rheumatoid arthritis (one; Fig. 1a). The median time to prepare the T cells for reinfusion based on 17 patients was 25 d (range, 17–40 d). The median number of T cells for each infusion per patient was $1.33\times10^9$ (range, $0.48\times10^9$ to $2.38\times10^9$).

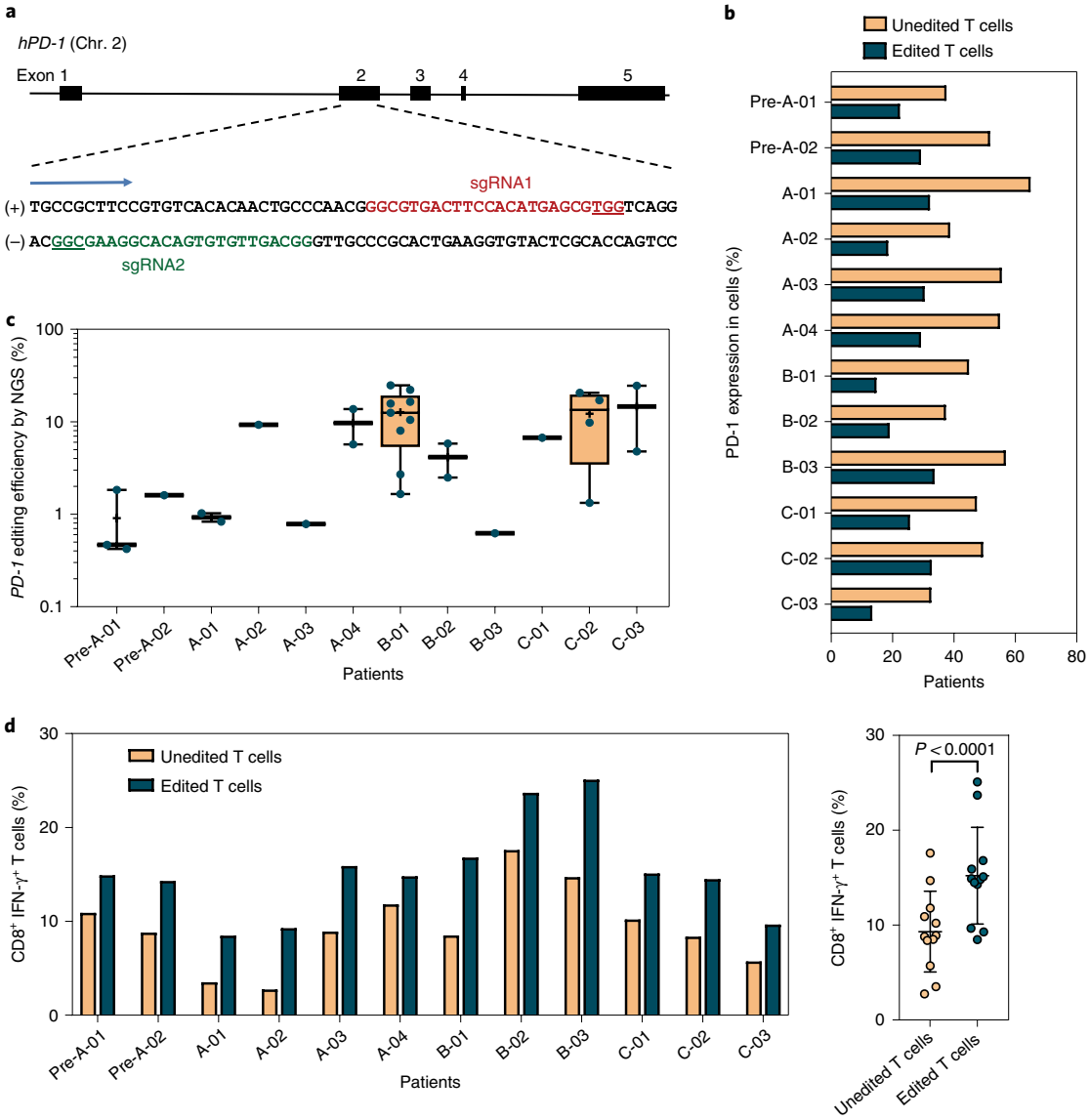


**Fig. 2 | CRISPR–Cas9-mediated *PD-1* gene editing in T cells. a**, The pair of sgRNAs (sgRNA1 and sgRNA2) that was designed to target exon 2 of *PD-1*. The PAM sequences are marked with an underscore. The Cas9 and sgRNA plasmids were cotransfected into T cells by electroporation. **b**, The levels of PD-1 expression on edited T cells or unedited T cells in the first cycle were measured by flow cytometry. **c**, The frequency of *PD-1* editing efficiency on all infused T cells was measured by NGS. Box-and-whisker plot shows the frequency of *PD-1* editing efficiency; the box represents the values from lower quartile to upper quartile, the center line in the box represents the median data and the whiskers (vertical) lines outside the box represent the minimum and maximum values. Each dot represents the editing efficiency of infused cells in an individual cycle. *n* represents the number of tested samples (patient ID); $n=1$ (pre-A-02, A-02, A-03, B-03 and C-01), $n=2$ (A-01, A-04, B-02 and C-03), $n=3$ (pre-A-01), $n=4$ (C-02), $n=9$ (B-01). **d**, The percentages of $CD8^+$ IFN-$\gamma^+$ cells in edited or unedited T cells on the first cycle were measured by flow cytometry (left panel), and analyzed by two-tailed paired *t*-test (right panel, $n=12$ per group, normally distributed data, each dot represents individual data from each patient, center line and error bar represent mean ± s.d., mean of differences = 5.896, 95% CI of difference, 4.602–7.189, degrees of freedom = 11, $P<0.0001$). Data are representative of three independent experiments. Chr., chromosome.

**Preparation and evaluation of edited T cells.** A pair of single guide RNAs (sgRNAs; sgRNA1 and sgRNA2) was selected to target exon 2 of the *PD-1* gene (Fig. 2a). The Cas9 and sgRNA plasmids were cotransfected into T cells by electroporation[14], which was established as the standard procedure for this trial in 2015. Since the launch of our trial, the superior CRISPR–Cas9 ribonucleoprotein (RNP) delivery platform has been developed[15]. However, to maintain consistency with our preliminary data on quality and stability of cellular therapy, we chose to continue with the plasmid system. Editing efficiency (median, 20.1%; range, 8.7–31.2%) was detectable by T7E1 cleavage surveyor assay (Extended Data Fig. 1a). Flow cytometric analysis revealed markedly decreased PD-1 expression, with median disruption of 46.3% (range, 33.7–67.0%) in edited T cells (Fig. 2b). TA-clone sequencing showed that the median *PD-1* gene-editing efficiency was 16% (range, 8–34%) in the first cycle (Extended Data Fig. 1b). NGS targeted sequencing of the *PD-1* gene using two rounds of PCR amplification was performed for further validation. The median editing efficiency of all 12 patients was 5.81% (range, 0.42–24.85%) (Fig. 2c). In edited T cells, most cells were CD3 positive (median, 99.1%; range, 95.9–99.6%), with CD3CD8 double-positive T cells accounting for 73.5% (range, 38.5–93.0%) (Supplementary Table 1). A significant increase in the

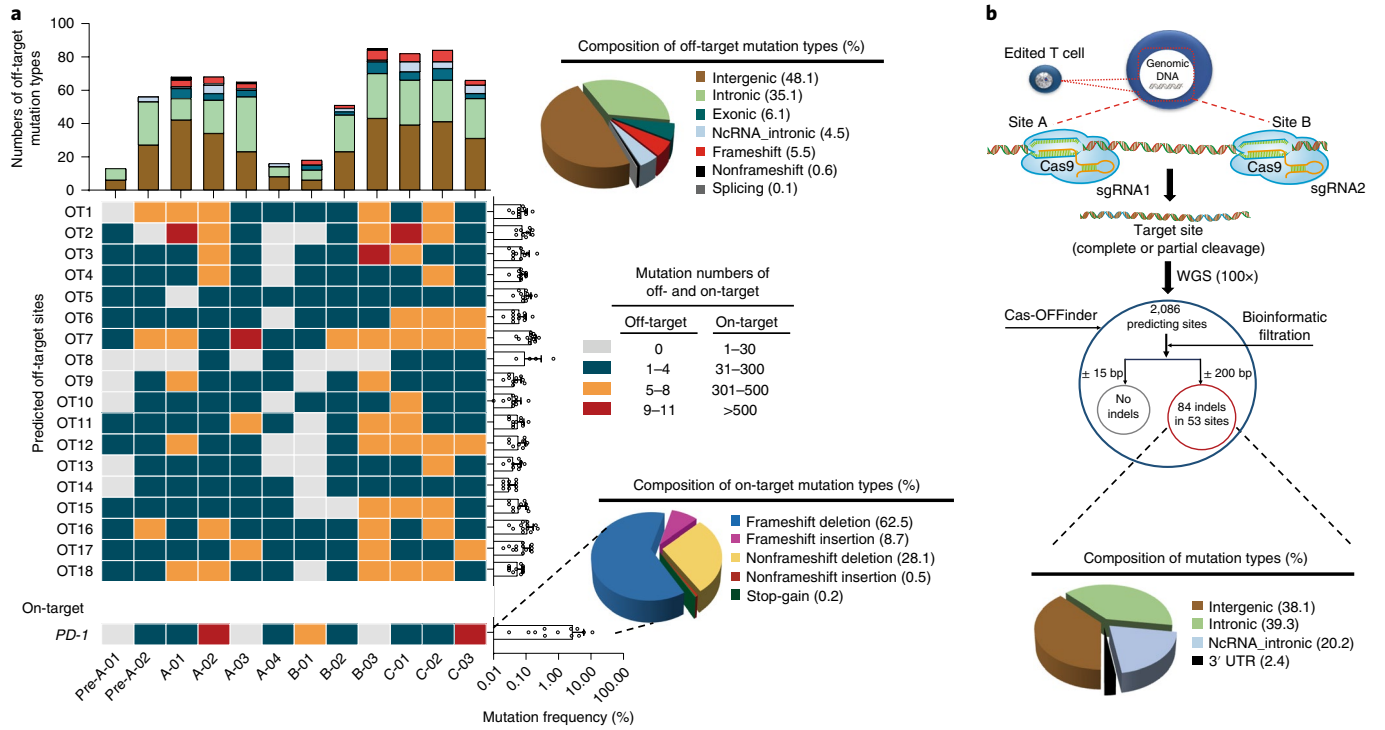


**Fig. 3 | Off-target analysis by NGS and WGS. a**, Characteristics of off-target mutation types, frequencies and numbers determined by NGS for the edited T cells of 12 enrolled patients before the first cycle of infusion. Bar graph and pie graph above represent the types, the numbers and the composition of off-target mutations, color-coded according to the legend to the right. Intergenic (48.1%) and intronic (35.1%) mutations composed the majority proportion. Heatmap shows the mutation number of predicted off-target sites (18 off-target sites, OT1–18) and on-target sites for individuals. Bar graph on the right represents mean mutation frequencies of each site among all of the patients (bars represent mean ± s.d., each dot represents individual data, $n = 12$). The modification ratio of on-target/off-target was 48.7. Pie graph on bottom right shows the composition of on-target mutation. The mutation types of on-target consisted of frameshift or nonframeshift (deletion/insertion mutation) and stop-gain mutations, while the vast majority were deletion mutations (90.6%). **b**, The genome DNA assessed by WGS (100×). From 19 samples for infusion from 12 patients, 2,086 potential off-target sites predicted by Cas-OFFinder were further analyzed by bioinformatics filtration. Indel events were not detected within 15 bp up- and downstream (±15 bp) of the sites. When each site was broadened to 200 bp up- and downstream (±200 bp), 84 indel events in 53 sites were detected. All of the indels were of 1 bp length variance on nucleotide repeats and thus were not considered to be true off-target events. Pie graph represents the types and the composition of 84 indel events. Intergenic (38.1%) and intronic (39.3%) mutations composed the majority proportion. NcRNA, Non-coding RNA; 3′ UTR, 3′ untranslated region.

proportion of $CD8^+IFN\text{-}\gamma^+$ cells was found in edited T cells compared with unedited cells ($P < 0.0001$) (Fig. 2d). Long-term culture experiments showed a dramatically higher capacity for stable viability (>90%) and expansion number in edited T cells (versus unedited cells) over 30–40 d from patients B-01 and C-02 (Extended Data Fig. 2).

To study the off-target impact of CRISPR–Cas9 on edited T cell genomes, we used sgRNAcas9 (v.2.0.6)[16] to predict the 18 potential off-target (OT) sites (labeled as OT1–18, representing sites 1–18), which would indicate the top candidates for off-target activity (based on sequence homology to the *PD-1*-targeting guide RNA) (Supplementary Tables 2 and 3). We performed NGS with cSMART (circulating single-molecule amplification and resequencing technology)[17] to detect off-target mutation frequencies and types, and their relative distributions of edited T cells infused in the first cycle (Fig. 3a) and the second cycle (Extended Data Fig. 3). The median mutation frequency of all off-target sites was 0.05% (range, 0–0.25%), which was much lower than that of the on-target site (median, 1.69% with *PD-1*; range, 0.03–11.08%). The modification ratio of on-target/off-target was 48.7. Mutation types such as frameshift indels (71.2%) and nonframeshift indels (28.6%) were mainly detected in on-target sites rather than off-target sites. In the predicted off-target sites, intergenic (48.1%) and intronic (35.1%) mutations composed a large proportion (Fig. 3a). The off-target effect was further assessed in seven samples of edited T cells infused in the second cycle, showing similar results. The modification ratio of on-target/off-target was 105.2 (Extended Data Fig. 3). Considering the limitation on the width of coverage by NGS, we have also performed WGS at 100× coverage using Cas-OFFinder[18] for identification of potential off-target sites. This method is an unbiased and direct method for extensive mutation searching. Contrarily, Guide-seq[19] is affected by considerable false negatives despite its high sensitivity[20]. In the current study, a total of 2,086 potential off-target sites were predicted by Cas-OFFinder. Indel events were not detected within 15 base pairs (bp) up- and downstream of the sites. When each site was broadened to 200 bp up- and downstream, 84 indel events in 53 sites were detected (Supplementary Table 4). All indel events were of 1-bp length variance on nucleotide repeats and thus were not considered to be true off-target events (Fig. 3b). There was a discrepancy in detectable off-target events between NGS and WGS, which we hypothesize is due to the differences in coverage of sequencing. Compared with NGS, WGS has the ability to detect potential off-target sites with higher frequency[20]. However, due to the limitations of our methodology, absence of detectable off-target sites does not entirely rule out off-target events.

**Safety and clinical outcomes.** The first patient in the pre-A cohort (pre-A-01) developed grade 1 arrhythmia, detected as a premature beat on electrocardiography at day 1 of cell infusion. Cardiac evaluation, including myocardial enzyme test (creatine kinase-MB,

**Table 1 | Summary of treatment-related AEs**

| AE[a] grade (%) | Total | | | | Cohort | | | | | | | | | | |
|---|---|---|---|---|---|---|---|---|---|---|---|---|---|---|---|
| | (*n* = 12) | | | | Pre-A (*n* = 2) | | | A (*n* = 4) | | | B (*n* = 3) | | | C (*n* = 3) | | |
| | Total | 1 | 2 | ≥3 | 1 | 2 | ≥3 | 1 | 2 | ≥3 | 1 | 2 | ≥3 | 1 | 2 | ≥3 |
| Any event | 11 (92) | 8 (67) | 3 (25) | 0 | 2 (100) | 0 | 0 | 3 (75) | 1 (25) | 0 | 2 (67) | 1 (33) | 0 | 1 (33) | 1 (33) | 0 |
| Lymphopenia | 3 (25) | 2 (17) | 1 (8) | 0 | 1 (50) | 0 | 0 | 0 | 0 | 0 | 1 (33) | 0 | 0 | 0 | 1 (33) | 0 |
| Fatigue | 3 (25) | 3 (25) | 0 | 0 | 1 (50) | 0 | 0 | 0 | 0 | 0 | 2 (67) | 0 | 0 | 0 | 0 | 0 |
| Leukopenia | 2 (17) | 1 (8) | 1 (8) | 0 | 0 | 0 | 0 | 1 (25) | 0 | 0 | 0 | 1 (33) | 0 | 0 | 0 | 0 |
| Fever | 2 (17) | 2 (17) | 0 | 0 | 0 | 0 | 0 | 0 | 0 | 0 | 2 (67) | 0 | 0 | 0 | 0 | 0 |
| Arthralgia | 2 (17) | 2 (17) | 0 | 0 | 0 | 0 | 0 | 1 (25) | 0 | 0 | 1 (33) | 0 | 0 | 0 | 0 | 0 |
| Rash | 2 (17) | 2 (17) | 0 | 0 | 1 (50) | 0 | 0 | 1 (25) | 0 | 0 | 0 | 0 | 0 | 0 | 0 | 0 |
| Neutropenia | 1 (8) | 0 | 1 (8) | 0 | 0 | 0 | 0 | 0 | 0 | 0 | 0 | 1 (33) | 0 | 0 | 0 | 0 |
| Infusion-related reaction | 1 (8) | 0 | 1 (8) | 0 | 0 | 0 | 0 | 0 | 1 (25) | 0 | 0 | 0 | 0 | 0 | 0 | 0 |
| Hyperhidrosis | 1 (8) | 1 (8) | 0 | 0 | 0 | 0 | 0 | 0 | 0 | 0 | 1 (33) | 0 | 0 | 0 | 0 | 0 |
| Premature beats[b] | 1 (8) | 1 (8) | 0 | 0 | 1 (50) | 0 | 0 | 0 | 0 | 0 | 0 | 0 | 0 | 0 | 0 | 0 |
| Hypertension | 1 (8) | 1 (8) | 0 | 0 | 1 (50) | 0 | 0 | 0 | 0 | 0 | 0 | 0 | 0 | 0 | 0 | 0 |
| Increased AST | 1 (8) | 1 (8) | 0 | 0 | 0 | 0 | 0 | 1 (25) | 0 | 0 | 0 | 0 | 0 | 0 | 0 | 0 |
| Increased ALT | 1 (8) | 1 (8) | 0 | 0 | 1 (50) | 0 | 0 | 0 | 0 | 0 | 0 | 0 | 0 | 0 | 0 | 0 |
| Thrombocytopenia | 1 (8) | 1 (8) | 0 | 0 | 0 | 0 | 0 | 0 | 0 | 0 | 1 (33) | 0 | 0 | 0 | 0 | 0 |
| Anemia | 1 (8) | 1 (8) | 0 | 0 | 0 | 0 | 0 | 0 | 0 | 0 | 0 | 0 | 0 | 1 (33) | 0 | 0 |

All data are presented as *n* (%). ALT, alanine aminotransferase; AST, aspartate aminotransferase. [a]Listed are events that were considered to be related to treatment by the investigator; number of patients with treatment-related AEs was recorded after the initiation of cell infusion. These were all grade 1 or 2. [b]The patient had both junctional and ventricular premature beats.

troponin T and myoglobin), and echocardiography were normal (Extended Data Fig. 4). This patient received the second and third infusions on days 3 and 5, and no dose-limiting toxicities (DLTs) were observed. The second patient of the pre-A cohort (pre-A-02) did not experience any DLT. Per protocol, a total of ten patients were enrolled in dose-escalation cohorts A–C (Fig. 1b). At the time of data cut-off (31 January 2020), a total of 37 infusions were given to the enrolled patients. Patients' characteristics are summarized in Extended Data Fig. 5.

Grade 1/2 treatment-related adverse events (AEs) occurred in 11 of the 12 patients, and no AEs occurred in patient C-03 (Table 1). There were no grade ≥3 treatment-related AEs. Details of AEs are summarized in Supplementary Table 5. Common treatment-related AEs included lymphopenia (*n* = 3, 25%), fatigue (*n* = 3, 25%), leukopenia (*n* = 2, 17%), fever (*n* = 2, 17%), arthralgia (*n* = 2, 17%) and skin rash (*n* = 2, 17%). Other treatment-related AEs included neutropenia, infusion-related reaction, hyperhidrosis, premature beats, hypertension, increased alanine aminotransferase, increased aspartate aminotransferase, thrombocytopenia and anemia (*n* = 1, 8%, Table 1). Duration of treatment-related AEs is shown in Extended Data Fig. 6, and the more durable AEs included arthralgia (52.4 weeks), premature beats (19.1 weeks) and fatigue (15.3 weeks). Serum cytokine analysis was done for all patients, and none of the patients had evidence of cytokine release syndrome (Fig. 4a). No DLTs were observed. During the follow-up for safety (up to 2 yr after the last treatment), 3 of the 12 patients had grade 1 treatment-related AEs (Extended Data Fig. 7).

Among the enrolled 12 patients, the median progression-free survival (PFS) was 7.7 weeks (95% confidence interval (95% CI), 6.9–8.5 weeks). The median overall survival (OS) was 42.6 weeks (95% CI, 10.3–74.9 weeks) (Extended Data Fig. 8). The median follow-up was 47.1 weeks (range, 13.4–116.0 weeks). One patient was unavailable for assessment of efficacy due to early withdrawal. None of the patients attained partial response and two patients had stable disease (Fig. 4b). The 8-week disease control rate was 16.7% (2 of 12; 95% CI, 2.1–48.4%). As of 31 January 2020, all patients had disease progression. Of 12 patients, 11 (91.7%) died from tumor progression. The one remaining patient (C-02) was still receiving other therapy (Fig. 4c). No treatment-related death occurred in our study.

**In vivo tracking of edited T cells.** To monitor the in vivo persistence of edited T cells after infusion, we used NGS to detect the disrupted *PD-1* gene in DNA extracted from blood samples of treated patients per protocol. Presence of the edited *PD-1* gene in PBMCs, acting as a surrogate for gene-edited T cells, was detected in 11 of the 12 treated patients (patient A-03 was not available for testing due to early withdrawal) at multiple time points between 8.0 and 52.0 weeks from the first infusion, and the allele frequency of edited *PD-1* gene varied among the patients. Interestingly, one patient (B-01) with durable disease control showed a persistent, moderate level of edited *PD-1* genes in PBMCs (Fig. 4d).

**Peripheral TCR clonal diversity.** High TCR diversity in PBMCs is associated with better response to immune checkpoint inhibitor (ICI) treatment[21]. The Shannon diversity index was calculated using TCR clonality of PBMCs from healthy donors and patients with refractory NSCLC. The median index of TCR clone diversity was significantly lower in our 12 treated patients at baseline than in healthy donors, with 5.65 (range, 2.22–7.44) and 8.11 (range, 5.17–8.86) ($P = 0.0005$), respectively (Extended Data Fig. 9). The TCR clone diversity was detectable in all patients and we observed a trend toward increased diversity over time in one patient (Fig. 4e). The median index was 6.54 (range, 2.56–8.29) at week 8, 7.05 (range, 6.48–8.57) at week 20 and 8.33 at week 68 following cell therapy.

We also tracked unique TCR clones by performing NGS of the complementarity-determining region 3 (CDR3). Unique TCR clones were defined as TCR clones that were undetectable in baseline PBMCs, but became detectable after the first infusion of gene-edited T cells. We observed that the unique clones were

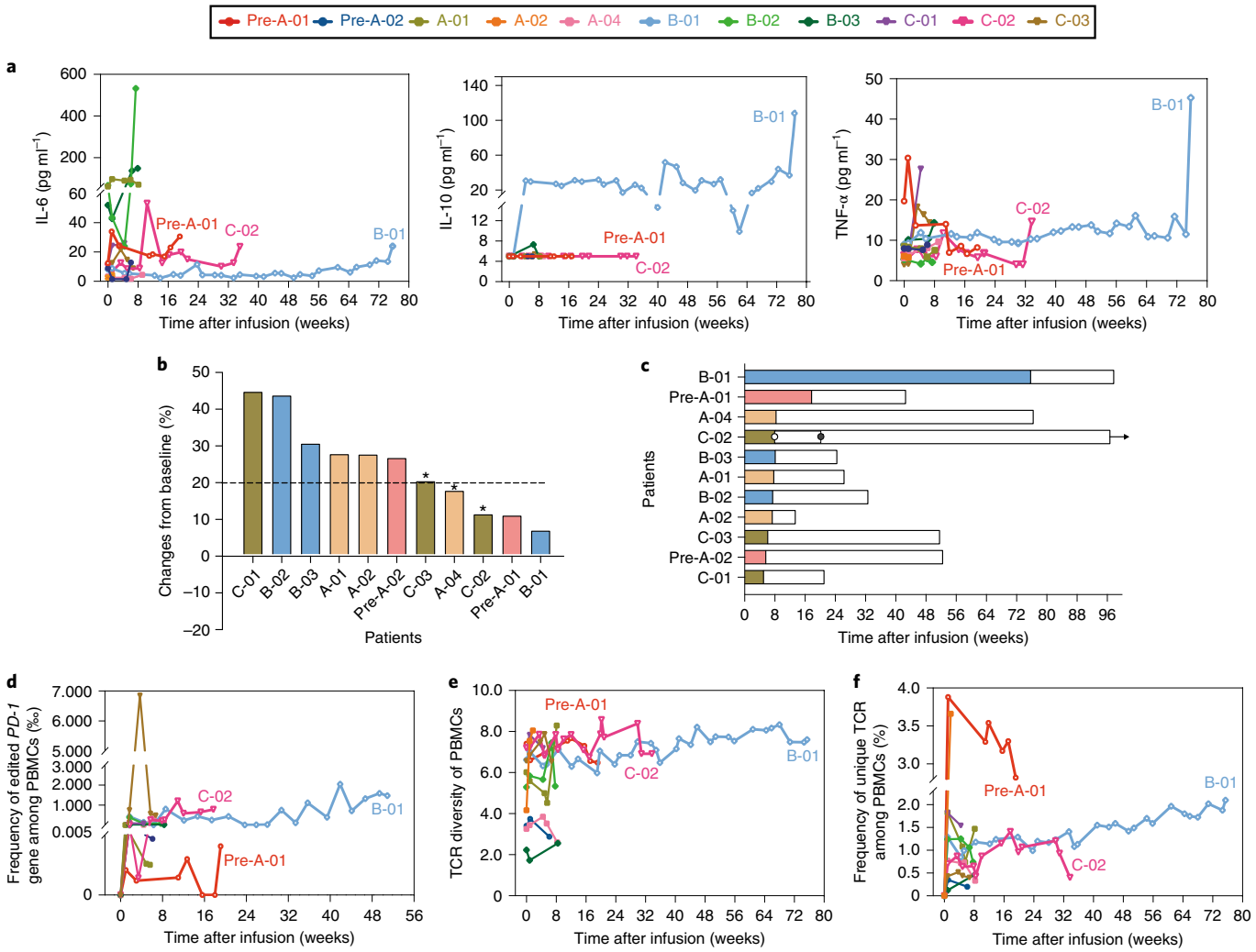


**Fig. 4 | Persistence, TCR clones, cytokines and clinical outcomes of patients who received therapy with the gene-edited T cells. a**, Changes in IL-6 (left), IL-10 (middle) and tumor necrosis factor alpha (TNF-α) (right) in all patients during and after treatment. **b**, Bar graph representation of best percentage change from baseline tumor size, as determined based on Response Evaluation Criteria in Solid Tumors (RECIST), v.1.1. The dashed line represents the cut-off for PD (at 20% change in tumor size from baseline). An asterisk denotes PD with new lesions. **c**, Swimmer plot represents the treatment duration for 11 patients. Arrow represents that the patient was alive at the time of date cut-off (31 January 2020). Color bar represents the PFS time; blank bar represents the survival time after PD. Hollow and solid dots represent that patient C-02 experienced only intracranial progression and then intrapulmonary lesion PD, respectively. **d**, Frequency of edited *PD-1* gene in PBMCs of each patient based on NGS from the time of first-cycle cell infusion up to 1 yr. **e**, TCR diversity of patients' PBMCs collected at different time points during therapy. **f**, Frequency of unique TCR clones among patients' PBMCs during the course of the trial. The unique TCR clones were defined as the different clones of only edited T cells in PBMCs after the first treatment from PBMCs of the baseline.

detected in all patients on day 6 and at week 8 after the first infusion with median frequency of 1.01% (range, 0.12–3.88%) and 0.74% (range, 0.33–3.29%), respectively. These TCR clones were detectable until week 76 in patient B-01 (Fig. 4f).

**Clinical outcome of patient B-01.** Patient B-01 had stable disease lasting for 76 weeks. This 55-yr-old woman had metastatic lung adenocarcinoma with positive PD-L1 expression (tumor proportion scores of 5%). She had failed three lines of treatment before infusion. At 8 weeks after the first T cell infusion, she developed pleural effusion which spontaneously resolved in 4 weeks without intervention. Positron emission tomography–computed tomography at 52 weeks showed only one tumor site with increased metabolic uptake (Fig. 5a). Four re-biopsy specimens were collected (before treatment, post-treatment weeks 24 and 54, and at tumor progression at week 76). Biopsy analysis revealed that there was minimal residual tumor, and increased infiltrating T cells (CD3+/CD8+ T cells) and CD68+ macrophages, at week 54 compared with the baseline, while the infiltrating T cells were hardly detected at tumor progression (Fig. 5b; semiquantitative analysis of staining density is presented in Extended Data Fig. 10).

The median *PD-1* editing efficiency of infused T cells from patient B-01 was 12.50% (range, 1.65–24.85%). The frequency of edited *PD-1* gene detected in PBMCs was similar to the editing efficiency of infused T cells (Fig. 5c). This patient had persistent unique TCR clones and TCR diversity in the peripheral blood during the 17.5 months of clinical follow-up (Fig. 5d). Notably, the TCR clones with high frequency (≥0.1%) in tumors changed greatly during treatment and were also correspondingly detectable in the PBMCs (Fig. 5e,f). We further explored the shared TCR clones between tumor tissue and the edited T cells in this patient. Interestingly, the high-frequency clones (defined as ≥0.1%) in the tumor composed the majority (82%) of the shared TCR clones between tumor and the edited T cells at baseline (Fig. 5g). The numbers of shared clones

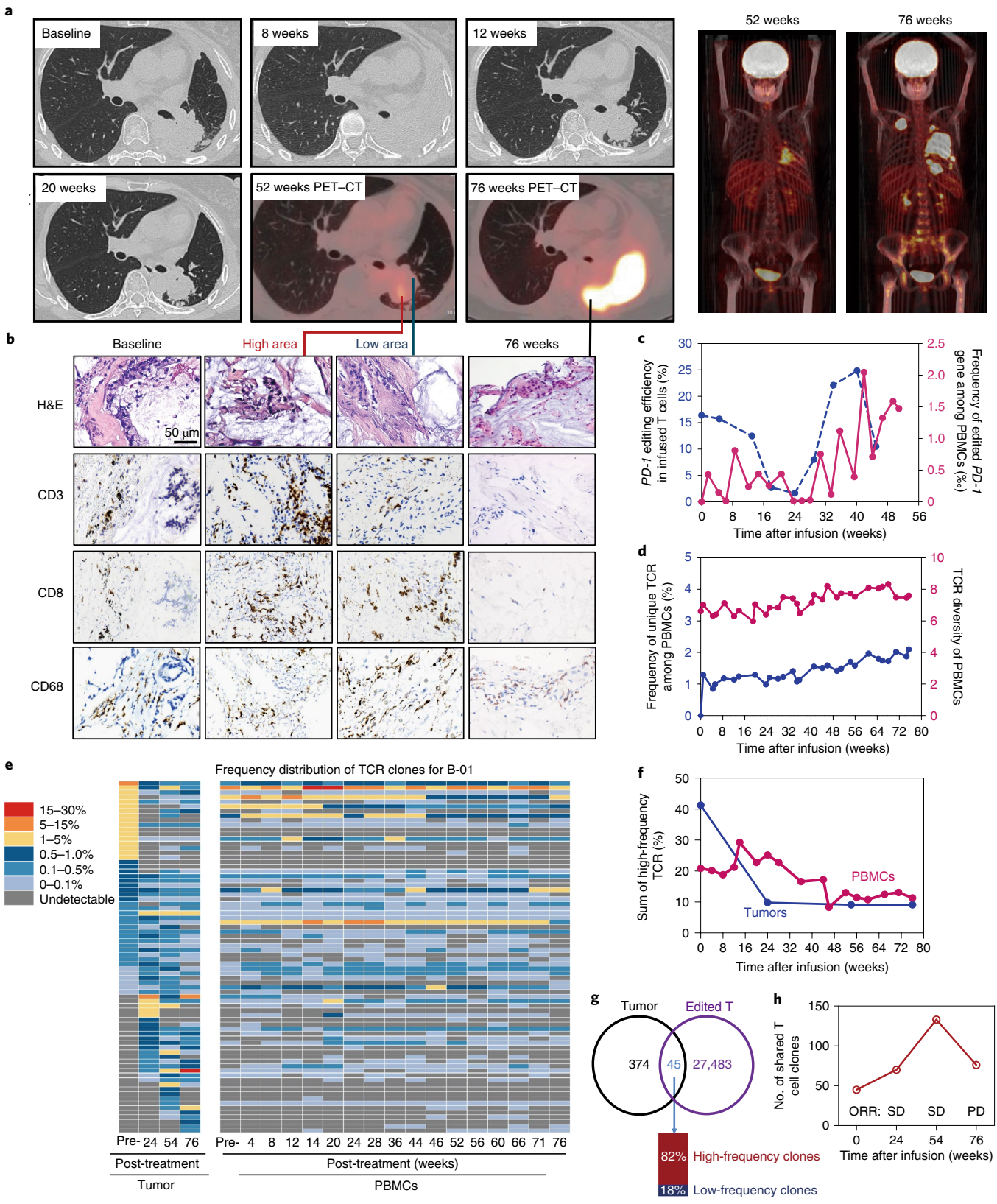


increased by week 24 and week 54 during stable disease, and then declined at week 76 with disease progression (Fig. 5h).

## Discussion

Our study further supports the safety and feasibility of gene-edited T cell therapy by CRISPR–Cas9 technology in the clinic, in line with data from another recently published clinical trial[6]. The final dose is $4\times10^7$ T cells per kg given in a 28-d cycle. All treatment-related AEs were grade 1 or 2, and the more frequent events included lymphopenia, fatigue, leukopenia, fever, arthralgia and skin rash. Severity of AEs appeared to be dose-independent (Table 1). Only one patient had grade 1 arrhythmia after the first infusion, lasting 19.1 weeks

**Fig. 5 | Outcomes of B-01. a**, Computerized tomography (CT) and positron emission tomography (PET) images of patient B-01. The patient underwent radiological imaging before T cell infusion (baseline) and at weeks 8, 12, 20, 52 and 76 after the first cycle of T cell infusion. Left pleural effusion developed at week 8, and then resolved at week 12 without any intervention. **b**, Representative photo micrographs showing histological staining of tumor specimens from patient B-01. At 54 weeks after cell infusion, tumor biopsies were performed in the high-metabolism and low-metabolism areas. Tumor re-biopsy was performed at tumor progression at week 76. Sections were stained, as indicated, with hematoxylin-eosin (H&E) or with immunohistochemistry antibodies directed against CD3, CD8 and CD68. Data are representative of three separate slides. Magnification, ×400. **c**, *PD-1* editing efficiencies in preinfusion edited T cells (left axis) and postinfusion PBMCs (right axis) at different time points in patient B-01 were measured by NGS. **d**, Frequency of unique TCR clones among PBMCs (left axis) and TCR diversity of PBMCs (right axis) during therapy were measured by NGS. **e**, Heatmap represents the frequency distribution of TCR clones in the tumors and PBMCs at indicated time points. The top 20 TCR clones detected in four tumor samples and the overlapped clones among tumor samples were included for this analysis. Each colored bar represents a unique CDR3, and each color denotes the CDR3 frequency in each sample. The T cell repertoire in the tumor changed substantially during T cell therapy. The TCR clones abundant in baseline tumor were also found in the PBMCs after cell treatment. **f**, Sum of high-frequency TCR clones in the tumors of patient B-01 at baseline and post-treatment (weeks 24, 54 and 76 after cell treatment), and PBMCs at indicated time points. High-frequency clones were defined as those with abundance ≥0.1% in tumor tissue. **g**, The number of shared TCR clones between the tumor tissue and edited T cells (Venn diagram). The proportions of shared TCR clones with high frequency (≥0.1%) and low frequency (<0.1%) in tumor tissue at baseline (below bar). The high-frequency clone (≥0.1% in tumor) composed the majority (82%) of shared clones at the baseline. **h**, Changes in shared TCR clones from patient B-01 at baseline and weeks 24, 54 and 76 after cell treatment. Patient B-01 experienced tumor progression at week 76. ORR, objective response rate; SD, stable disease.

(Extended Data Fig. 6), but the causal relationship to treatment is uncertain. We speculate that lymphocyte infiltration to the myocardium occurred in this patient, which is a known but rare complication of immune checkpoint inhibitors such as ipilimumab and nivolumab[22], but we do not have sufficient evidence to confirm the causal relationship.

Off-target editing by the CRISPR–Cas9 system is a major concern for clinical application of the technology. Off-target events were not detected in a patient who received CRISPR-edited stem cell therapy[5]. For three patients treated with multigene-edited T cell therapy, there were minimal off-target events at *TRAC* and *TRBC*[6]. Similarly, our median mutation frequency of off-target cleavage was low in all sites by NGS, with the majority of these mutations being located in intergenic or intronic regions (Fig. 3a), which were unlikely to have significant effects on coding genes. Frameshift or nonframeshift mutations (insertion/deletion mutations) caused by CRISPR–Cas9 technology may induce gene dysfunction[23,24]. The mean frequencies of frameshift and/or nonframeshift mutations in the predicted sites appeared to be low, by both 20,000× NGS coverage (Fig. 3a) and 100× WGS coverage (Fig. 3b). We adopted the plasmid electroporation strategy, while the recent publication from the United States used RNP editing[6]. It appears that both strategies are associated with low incidence of off-target events, but this should be verified in future studies.

The persistence of edited T cells in the periphery and intratumorally could support the potential efficacy of the gene-edited T cells[25,26]. The disrupted *PD-1* gene and unique TCR clones were detectable at 4 weeks in all patients, while the finding was more persistent in patients with stable disease (pre-A-01, B-01) (Fig. 4d,f). Notably, the high-frequency clones (≥0.1%) had a decreasing trend both in tumor and in PBMCs (Fig. 5f). Given these data and that the more frequent TCR clones are likely reactive to tumor neoantigens[27], we postulate that the edited T cells were capable of recognizing tumor neoantigens. However, limited by the small sample size of the study, this hypothesis can only be validated in a future study.

We did not observe objective responses in this cohort of heavily treated patients. Several factors, including insufficient T cell expansion, lack of antigen specificity and/or tumor cells not being PD-L1 dependent, may account for the low response rate. While we did confirm that all enrolled patients had PD-L1$^+$ tumors, PD-L1 expression by immunohistochemistry does not necessarily correlate with PD-L1 dependency. Five of the enrolled patients could not participate as a result of insufficient T cell expansion ex vivo. During primary cell culture and editing, some of the well-transformed cells failed to proliferate. This could be related either to poor quality of T cells from heavily treated patients or to the manufacturing procedure. Comparatively, in four of six patients whose T cells were manufactured by RNP editing, sufficient cell product was successfully obtained[6]. It is possible that the lack of tumor response was related to T cell anergy or exhaustion resulting from chronic exposure to tumor-associated antigens or anti-cancer therapy[28]. Unlike other cancer types, including melanoma and sarcoma and virus-related malignancies, there are currently no promising target antigens for lung cancer. Our study used T cells from peripheral blood for gene editing, which may include tumor-reactive T cells[29]. However, efficacy may be limited in patients with low frequencies of tumor-reactive T cells. Future clinical trials should use improved quantities of tumor-reactive or tumor antigen-specific T cells.

We used nucleofection to deliver plasmids encoding Cas9 and sgRNA into primary T cells to disrupt genomic *PD-1* expression. A potential benefit of this approach is shorter exposure of the editing genomic components to the target cell, which may reduce the risk of off-target mutations[30]. However, this method may be associated with low editing efficiency. It is important to note that the editing protocol for the cells used in the current trial was based on the reagents available in 2015. Other technologies developed since the launch of our trial, such as RNA encoding the Cas9 and sgRNA[31], Cas9 RNPs[32], Cas9 messenger RNA or protein with chemically modified sgRNA[33], may result in improved editing efficiencies. Using nucleofection, the median editing efficiency for PD-L1 was 5.81% (range, 0.42–24.85%). In contrast, using RNP editing for *TRAC*, *TRBC* and *PDCD1*, the editing efficiency was 45%, 15% and 20%, respectively[6]. The new approach appears to have advantage in editing efficiency over plasmid nucleofection. Our study has confirmed the safety and feasibility of gene-edited T cell therapy, while we anticipate that the higher editing efficiency with RNP editing would further improve the treatment efficacy.

We should emphasize that the long-term safety of clinical use of CRISPR–Cas9 technology remains important. After a median follow-up of 47.1 weeks (range, 13.4–116.0 weeks) as of 31 January 2020, none of the 12 patients had treatment-related severe AEs (Extended Data Fig. 7). The same was observed in the three patients who received RNP gene-edited T cells, but their duration of follow-up was much shorter[6]. We performed the gene-editing process ex vivo and demonstrated that the lifespan of the gene-edited T cells was short (Supplementary Fig. 1), suggesting that the risk of permanent genomic alteration is limited.

In summary, this study has demonstrated the safety and feasibility of CRISPR–Cas9 gene-edited T cell therapy targeting the *PD-1* gene in a cohort of patients with advanced lung cancer. There were limited off-target effects observed with this approach, and we have demonstrated CRISPR-based technology to be clinically

feasible. However, considering the limitations of the technology used in the study, future trials should use newer and more effective gene-editing systems.

## Online content

Any methods, additional references, Nature Research reporting summaries, source data, extended data, supplementary information, acknowledgements, peer review information; details of author contributions and competing interests; and statements of data and code availability are available at https://doi.org/10.1038/s41591-020-0840-5.

Received: 25 September 2019; Accepted: 18 March 2020;
Published online: 27 April 2020

## References

1. Cong, L. et al. Multiplex genome engineering using CRISPR/Cas systems. *Science* **339**, 819–823 (2013).
2. Jinek, M. et al. A programmable dual-RNA-guided DNA endonuclease in adaptive bacterial immunity. *Science* **337**, 816–821 (2012).
3. Hsu, P. D., Lander, E. S. & Zhang, F. Development and applications of CRISPR-Cas9 for genome engineering. *Cell* **157**, 1262–1278 (2014).
4. Kosicki, M., Tomberg, K. & Bradley, A. Repair of double-strand breaks induced by CRISPR–Cas9 leads to large deletions and complex rearrangements. *Nat. Biotechnol.* **36**, 765–771 (2018).
5. Xu, L. et al. CRISPR-edited stem cells in a patient with HIV and acute lymphocytic leukemia. *N. Engl. J. Med.* **381**, 1240–1247 (2019).
6. Stadtmauer, E. A. et al. CRISPR-engineered T cells in patients with refractory cancer. *Science* **367**, eaba7365 (2020).
7. Mok, T. S. K. et al. Pembrolizumab versus chemotherapy for previously untreated, PD-L1-expressing, locally advanced or metastatic non-small-cell lung cancer (KEYNOTE-042): a randomised, open-label, controlled, phase 3 trial. *Lancet* **393**, 1819–1830 (2019).
8. Reck, M. et al. Pembrolizumab versus chemotherapy for PD-L1-positive non-small-cell lung cancer. *N. Engl. J. Med.* **375**, 1823–1833 (2016).
9. Garon, E. B. et al. Five-year overall survival for patients with advanced nonsmall-cell lung cancer treated with pembrolizumab: results from the phase I KEYNOTE-001 Study. *J. Clin. Oncol.* **37**, 2518–2527 (2019).
10. Su, S. et al. CRISPR-Cas9-mediated disruption of PD-1 on human T cells for adoptive cellular therapies of EBV positive gastric cancer. *Oncoimmunology* **6**, e1249558 (2016).
11. Beane, J. D. et al. Clinical scale zinc finger nuclease-mediated gene editing of PD-1 in tumor infiltrating lymphocytes for the treatment of metastatic melanoma. *Mol. Ther.* **23**, 1380–1390 (2015).
12. Chen, W. et al. Cancer statistics in China, 2015. *CA Cancer J. Clin.* **66**, 115–132 (2016).
13. Bray, F. et al. Global cancer statistics 2018: GLOBOCAN estimates of incidence and mortality worldwide for 36 cancers in 185 countries. *CA Cancer J. Clin.* **68**, 394–424 (2018).
14. Su, S. et al. CRISPR-Cas9 mediated efficient PD-1 disruption on human primary T cells from cancer patients. *Sci. Rep.* **6**, 20070 (2016).
15. Schumann, K. et al. Generation of knock-in primary human T cells using Cas9 ribonucleoproteins. *Proc. Natl Acad. Sci. USA* **112**, 10437–10442 (2015).
16. Xie, S., Shen, B., Zhang, C., Huang, X. & Zhang, Y. sgRNAcas9: a software package for designing CRISPR sgRNA and evaluating potential off-target cleavage sites. *PLoS ONE* **9**, e100448 (2014).
17. Lv, W. et al. Noninvasive prenatal testing for Wilson disease by use of circulating single-molecule amplification and resequencing technology (cSMART). *Clin. Chem.* **61**, 172–181 (2015).
18. Bae, S., Park, J. & Kim, J. S. Cas-OFFinder: a fast and versatile algorithm that searches for potential off-target sites of Cas9 RNA-guided endonucleases. *Bioinformatics* **30**, 1473–1475 (2014).
19. Tsai, S. Q. et al. GUIDE-seq enables genome-wide profiling of off-target cleavage by CRISPR-Cas nucleases. *Nat. Biotechnol.* **33**, 187–197 (2015).
20. Manghwar, H. et al. CRISPR/Cas systems in genome editing: methodologies and tools for sgRNA design, off-target evaluation, and strategies to mitigate off-target effects. *Adv. Sci.* **7**, 1902312 (2020).
21. Robert, L. et al. CTLA4 blockade broadens the peripheral T-cell receptor repertoire. *Clin. Cancer Res.* **20**, 2424–2432 (2014).
22. Johnson, D. B. et al. Fulminant myocarditis with combination immune checkpoint blockade. *N. Engl. J. Med.* **375**, 1749–1755 (2016).
23. Sui, T. et al. CRISPR-induced exon skipping is dependent on premature termination codon mutations. *Genome Biol.* **19**, 164 (2018).
24. Cho, S. W. et al. Analysis of off-target effects of CRISPR/Cas-derived RNA-guided endonucleases and nickases. *Genome Res.* **24**, 132–141 (2014).
25. Kalos, M. & June, C. H. Adoptive T cell transfer for cancer immunotherapy in the era of synthetic biology. *Immunity* **39**, 49–60 (2013).
26. Rapoport, A. P. et al. NY-ESO-1-specific TCR-engineered T cells mediate sustained antigen-specific antitumor effects in myeloma. *Nat. Med.* **21**, 914–921 (2015).
27. Pasetto, A. et al. Tumor- and neoantigen-reactive T-cell receptors can be identified based on their frequency in fresh tumor. *Cancer Imunol. Res.* **4**, 734–743 (2016).
28. Zarour, H. M. Reversing T-cell dysfunction and exhaustion in cancer. *Clin. Cancer Res.* **22**, 1856–1864 (2016).
29. Dijkstra, K. K. et al. Generation of tumor-reactive T cells by co-culture of peripheral blood lymphocytes and tumor organoids. *Cell* **174**, 1586–1598. e1512 (2018).
30. Mandal, P. K. et al. Efficient ablation of genes in human hematopoietic stem and effector cells using CRISPR/Cas9. *Cell Stem Cell* **15**, 643–652 (2014).
31. Ren, J. et al. Multiplex genome editing to generate universal CAR T cells resistant to PD1 inhibition. *Clin. Cancer Res.* **23**, 2255–2266 (2017).
32. Kim, S., Kim, D., Cho, S. W., Kim, J. & Kim, J. S. Highly efficient RNA-guided genome editing in human cells via delivery of purified Cas9 ribonucleoproteins. *Genome Res.* **24**, 1012–1019 (2014).
33. Hendel, A. et al. Chemically modified guide RNAs enhance CRISPR-Cas genome editing in human primary cells. *Nat. Biotechnol.* **33**, 985–989 (2015).

**Publisher's note** Springer Nature remains neutral with regard to jurisdictional claims in published maps and institutional affiliations.

© The Author(s), under exclusive licence to Springer Nature America, Inc. 2020

## Methods

**Study design and patients.** This is a dose-escalating phase I clinical trial with four cohorts. In the pre-A cohort, we aimed to assure the safety of CRISPR-edited T cells to humans; a total of two patients received $2\times10^7$ edited T cells per kg body weight and were carefully monitored for 28 d (pre-A cohort). After assurance of the absence of significant toxicity, we started enrollment in the three-cohort dose-escalation study (cohorts A, B and C; Fig. 1b). With three subjects to each cohort, each patient received $1\times10^7$, $2\times10^7$ or $4\times10^7$ T cells per kg in a series of three infusions on days 1, 3 and 5, respectively. The first infusion contained 20% of the total number of cells; the second infusion, 30%; and the third infusion, 50%. At 3 d before the first infusion, cyclophosphamide (20 mg kg$^{-1}$) was given for lymphocyte depletion[34]. At day 28 from the first T cell infusion, and in the absence of major toxicity or disease progression, cycle 2 of the gene-edited T cell infusion would be administered, but without cyclophosphamide infusion. If the patients obtained clinical benefit, they would receive continuous treatment until unacceptable toxicity or withdrawal of consent, or disease progression. The unacceptable toxicity was defined as grade ≥3 cytokine release syndrome as well as grade ≥2 AE requiring systemic glucocorticoid therapy; in addition, patients would be withdrawn in the event of any AE, laboratory abnormality or intercurrent illness that the investigators judged would lead to great clinical risk in the patients.

Eligible patients were aged 18–70 yr and had histologically or cytologically confirmed stage IIIB or IV NSCLC[35]. Other major inclusion criteria included disease progression after three or more systemic therapies (including at least one molecular targeted therapy for patients with activating *EGFR* mutation or *ALK* fusion gene), positivity for PD-L1 expression as defined by tumor proportion score ≥ 1% using Ventana PD-L1 (SP142), adequate hematologic and organ functions, Eastern Cooperative Oncology Group score of 0–2 and a life expectancy of over 3 months. The re-biopsy samples were collected for exploratory analysis at the times of before treatment, half a year and 1 yr post-treatment, and at tumor progression if clinically feasible and agreed by patients. Key exclusion criteria were brain metastasis and/or spinal cord compression that were uncontrolled, active autoimmune disease, treatment with other immunomodulators within 28 d before the study and immunodeficiency. Complete eligibility criteria are provided in the study protocol (Supplementary clinical trial protocol). The patients were enrolled from 26 August 2016 to 21 March 2018.

The study protocol and subsequent amendments were approved by the Institutional Review Board of the West China Hospital, Sichuan University, Chengdu, China (2016 Review, No. 123). Written informed consent was obtained from all patients. Data were collected by the investigators. MedGenCell (Chengdu, China) provided the gene editing of T cells.

**Study endpoints and assessments.** The primary endpoints of this phase I dose-escalation study included safety and feasibility. Feasibility was defined by sufficient and viable (>90%) edited T cells being able to be manufactured from the majority (>50%) of enrolled patients. Secondary endpoints included objective response rate, 8-week disease control rate, PFS and overall survival. Other exploratory objectives included in vivo tracking of edited T cells, diversity and dynamics of TCR clones in PBMCs and re-biopsy tumor specimens (if available) and their potential correlations among efficacy outcomes.

All patients underwent baseline tumor assessment, including contrast-enhanced computed tomography and magnetic resonance imaging (MRI) of the brain, within 28 d before the first treatment. Tumor responses were assessed using Response Evaluation Criteria in Solid Tumors (RECIST 1.1) at weeks 8 and 12. Afterward, tumor responses were assessed every 8 weeks until disease progression or death.

AEs were monitored and graded according to the National Cancer Institute Common Terminology Criteria for Adverse Events (v.4.03) for 24 months after the last cell infusion or until the patient was lost to follow-up. AEs were identified using a predefined list of Medical Dictionary for Regulatory Activities (MedDRA, v.21.0) terms. DLTs were defined as events occurring within the first 28 d after the first cell infusion that required systemic glucocorticoids to be administered to patients, grade ≥2 autoimmune toxicities or any other grade ≥3 events, which were probably attributable to the T cell therapy. The association of AEs with treatment was determined by investigators.

**CRISPR plasmid construction.** To disrupt *PD-1* in human T cells we designed a pair of sgRNAs (sgRNA1 and sgRNA2), showing the highest editing efficiency in the 293 T cell line, to target exon 2 of *PD-1*. The Cas9 expression vector pST1374-Cas9 (Addgene) was constructed as previously described[14]. The *S. pyogenes* Cas9 (SpCas9) was used in the study. For the construction of the sgRNA vector, the single vector pGL3-hPD1 containing two sgRNAs was constructed as follows. Oligos for generation of sgRNAs were synthesized and annealed to form sgDNAs. Subsequently, the pGL3-dual U6 sgRNA scaffold-PGK-Puro vector (YouBio) was cleaved using restriction endonucleases. Finally, the sgDNAs were cloned one by one into the BsaI or BbsI sites of pGL3-dual U6 sgRNA scaffold-PGK-Puro vector, forming tandem dual sgRNA expression vectors. pGL3-dual U6 sgRNA scaffold-PGK-Puro vector was modified from pGL3-U6 sgRNA scaffold-PGK-Puro vector (Addgene).

**Preparation of *PD-1*-edited T cells.** *PD-1*-edited T cells were manufactured at MedGenCell (Chengdu, China). Briefly, PBMCs were isolated from 60–80 ml of peripheral blood from patients with NSCLC before every treatment cycle by centrifugation on a Ficoll density gradient. Approximately $5–10\times10^6$ cells were transfected by electroporation technology with the intended plasmids using a Nucleofector 2b device (Lonza) and the VPA-1002 Human T cells Nucleofector Kit (Lonza). After electroporation, cells were resuspended in X-VIVO15 medium (Lonza) containing 10% autologous serum with IFN-γ (2,000 IU ml$^{-1}$) and DNase (3 μg ml$^{-1}$) on day 1, and cultured with anti-CD3 antibody (0.4 μg ml$^{-1}$), anti-CD28 antibody (0.4 μg ml$^{-1}$) and interleukin-2 (IL-2) (1,000 IU ml$^{-1}$) from day 2 at 37 °C in a 5% $CO_2$ incubator. Cell culture medium was half-replaced every 2–3 d. Cell density was adjusted to $1–1.5\times10^6$ cells per ml. The final yield of cells was approximately $0.5–1.5\times10^9$ cells per bag with >95% cell viability at 20–28 d. The first and second cycles of cell infusion were conducted in the phase I clinical trial ward at West China Hospital, and the subsequent infusions were administrated in the inpatient ward at West China Hospital.

**T7E1 cleavage assay and sequencing.** To test the efficiency of *PD-1* gene editing, the T7E1 cleavage assay was performed as follows. Briefly, cells were collected and digested in lysis buffer (10 μM Tris-HCl, 0.4 M NaCl, 2 μM EDTA, 1% SDS and 100 μg ml$^{-1}$ Proteinase K). The genomic DNA was extracted by phenol-chloroform and precipitated using alcohol. Subsequently, targeted fragments of *PD-1* were PCR-amplified from genomic DNA using rTaq (Takara), and the PCR products were purified with a PCR cleanup kit (Axygen). The primer sequences for human *PD-1* are GTGGTGACCGAAGGGGACA (F) and GGATGACGTTACCTCGTGCG (R) from 5′ to 3′. Purified PCR products were denatured and re-annealed in NEBuffer 2 using the Veriti thermocycler (Applied Biosystems). Hybridized PCR products were digested with T7E1 (NEB) for 30 min and separated on 2% agarose gels. The purified PCR products were ligated with pEASY-T1 vector (TransGen Biotech). Ligation products were used for transformation and 50 colonies per transformation were sequenced using the universal primer M13F.

**Flow cytometry.** For detection of surface PD-1 expression, edited and unedited T cells were assessed by FACSAria II flow cytometry (BD Biosciences) after stimulation with anti-CD3/anti-CD28 Dynabeads (ThermoFisher Scientific). Cells were incubated with the following antibodies at room temperature in the dark for 30 min: CD3-BV510 (HIT3a, BD Biosciences), CD4-BV421 (RPA-T4, BD Biosciences), CD8-PE (HIT8a, BD Biosciences) and PD-1-APC (MIH4, BD Biosciences). For IFN-γ staining, cells were incubated with Leukocyte Activation Cocktail (BD Biosciences) and human PD-L1 protein (1 μg ml$^{-1}$, ACRO Biosystems) at 37 °C for 4 h. Then, cells were collected and washed, followed by staining with CD3-BV510 and CD8-APC-Cy7 at room temperature for 30 min. After fixation and permeabilization, cells were incubated with IFN-γ-PE (B27, BD Biosciences). Isotype staining was used as the negative control to determine the positive gate. Data were analyzed using FlowJo software (v.7.6.1). Editing efficiency (%) was calculated with the following equation: editing efficiency (%) = (PD-1-positive unedited cells (%) − PD-1-positive edited cells (%))/PD-1-positive unedited cells (%).

**Long-term cell culture.** To test whether *PD-1* disruption alters T cell viability or proliferation, the total cell number, viability and doubling time were assessed in a long-term culture. Cell culture medium was half-replaced every 2–3 d with fresh complete medium containing IL-2 (1,000 IU ml$^{-1}$), and cell density was stabilized at $1–1.5\times10^6$ cells per ml. The viability of *PD-1*-edited and -unedited T cells, cultured for 40 d, was evaluated with trypan blue staining.

**Detection of off-target sites by WGS analysis.** Genomic DNA was isolated from PBMCs and *PD-1*-edited T cells using QIAamp Circulating Nucleic Acid Kit (Qiagen). The whole-genome DNA library constructed using edited T cells and unedited T cells was sequenced on the NovaSeq 6000 platform (Illumina) with 100× coverage. We used samtools (v.1.1), sambamba (v.0.6.8), strelka2 (v.2.8.3) and Fusionmap (v.10.0.1.29) to process sequence alignment data (BAM file) and variant call format (VCF file), and then aligned each 150-bp sequenced read to the human reference genome (hg19) using Burrows–Wheeler Aligner (BWA, v.0.7.10) in the 'mem' mode ('BWA-MEM') with default parameters[36]. Reads caused by PCR duplication were labeled by sambamba[37], followed by strelka2 used for variants calling[38]. Lastly, all structure variant mutations were annotated with ANNOVAR (v.2019Oct24).

To predict potential off-target sites, we screened the whole human genome with the webtool Cas-OFFinder (v.2.4, http://www.rgenome.net/cas-offinder/). Any sequences within five mismatches (or fewer; a bulge penalty equals two base mismatches) of the two 20-nucleotide guide RNA sequences, followed by an NRG PAM, were called, and we obtained 2,086 sites[39]. Sequence alignment data (BAM files) were integrated by sambamba to call structure variants using strelka2 with default parameters[40] and to identify all translocations by Fusionmap. To get the candidate structure variants caused by off-target sites, we focused on insertion or deletion events (records contain 'FILTER = PASS' and 'INFO does not contain SNVHPOL information' in the VCF file) and filtered the indel events detected in

unedited samples. To further confirm whether off-target sites occurred among these sites, each event was broadened to 200 bp up- and downstream to intersect with 2,086 potential off-target sites. A total of 84 indel events in 53 sites were detected.

**Detection of off-target sites by NGS.** Potential off-target sites were predicted using sgRNAcas9 (v.2.0.6)[16]. The top 18 sites (that is, highest similarity to the targeted *PD-1* sequence) were considered potential off-target sites. Briefly, genomic DNA was isolated from *PD-1*-edited T cells with a QIAamp Circulating Nucleic Acid Kit (Qiagen). DNA was amplified by PCR for 14 cycles and further constructed DNA libraries. After denaturation of DNA to single strand, a bridging oligonucleotide synthesized with end sequences complementary to the PCR adaptors was used to facilitate ligation-mediated circularization with Taq ligase. The bridging oligonucleotide was also designed with a 7-bp NNNNNNN code and was synthesized as a mixture of degenerate molecules. The targeted regions within the circularized single-stranded molecules were amplified by inverse PCR using primer pairs located 16–29 bp apart.

In total, multiplexing of 36 inverse primer pairs was used to target mutation sites within the 18 locations. The pool of allelic molecules was subjected to pair-end sequencing on the NextSeq500 platform with 20,000× coverage of bases in the off-target sites. Finally, cSMART[17] was used for analysis and identification of point mutations and indels through the fastq join program (v.1.3.1, https://expressionanalysis.github.io/ea-utils/)[41]. The sequence reads were mapped to the human reference genome (hg19) using BWA-MEM. A minimum of one unique allelic read was used to define a read group with or without a mutation. Duplicate or higher-order reads with the same start and stop positions were distinguished by their unique barcodes and counted only once to correct PCR bias. The abundance of each mutation was expressed as the number of mutant molecules. For each region of potential off-target sequences, the number of unique allelic reads with mutations, the sum of fractions of each mutation and the fraction of indels in a specific region were calculated as the mutation rate of the given region. The number of unique allelic reads with deletions (Del) and insertions (Ins) of 1 bp or more are indicated. The indel frequency is the total number of unique allelic reads containing insertions and deletions for each off-target site expressed as a percentage of the total number of mapped unique allelic reads[42]. The primer pairs are listed in Supplementary Table 6.

The modification ratio of on-target/off-target was calculated as follows:

$$\mathrm{mR} = \frac{1}{18}\sum_{a=1}^{n} I_a\left(\frac{1}{\sum_{a=1}^{n} T_{1a}} + \frac{1}{\sum_{a=1}^{n} T_{2a}} + \ldots + \frac{1}{\sum_{a=1}^{n} T_{18a}}\right)$$

where mR represents the modification ratio of on-target/off target; $I_a$ represents the on-target frequency of patient number $a$; $n$ represents the number of patients; $T_{1a}$ represents the frequency of off-target site 1 (OT1) in patient number $a$; and $T_{18a}$ represents the frequency of off-target site 18 (OT18) in patient number $a$.

**Efficiency validation and in vivo tracking of edited T cells.** We performed assays of NGS targeting the *PD-1* gene on genomic DNA isolated from edited T cells and PBMCs using the QIAamp DNA Blood Mini Kit (Qiagen), and the DNA concentration was measured by Qubit dsDNA HS Assay Kit (Invitrogen). Thereafter, genomic regions of *PD-1* were amplified by PCR with primers homologous to the region of interest and the appropriate Illumina forward and reverse adapters (Supplementary Table 7). Primer pairs for the first round of PCR (PCR1) for all genomic sites can be found in Supplementary Table 8, and the optimal conditions of the PCR1 reaction were as follows: 0.5 µM forward primer, 0.5 µM reverse primer, 10 ng of genomic DNA and 10 µl of Phusion Hot Start Flex 2× Master Mix (NEB). Reactions were incubated for 2 min at 95 °C; 19 cycles of 10 s at 98 °C, 20 s at 65 °C and 15 s at 72 °C; followed by 2 min at 72 °C for extension. PCR products were verified by 2% agarose gel electrophoretic analysis and compared with DNA standards (Quick-Load 100-bp DNA ladder). Unique Illumina barcoding primer pairs were added to each sample for the secondary PCR reaction (PCR2), which was performed in a manner similar to PCR1. Finally, PCR products purified by AMPure XP beads (NEB) and quantified with an Agilent Bioanalyzer 2100 were sequenced on a HiSeq X Ten instrument (Illumina) following the manufacturer's protocols.

In brief, several steps, including demultiplexing of sequencing reads by MiSeq Reporter (Illumina), alignment of sequences by a modified version of MATLAB script and the Smith–Waterman algorithm and converting of bases (<30 of quality score) to *N*, were completed. Then, indels were quantified by the MATLAB script. After filtering out reads, insertion or deletion events of at least 2 bp within 30 bp up- or downstream of the Cas9 cleavage site were counted. Finally, the ratio of mutation reads to sequencing reads was calculated as the editing frequency of *PD-1* of edited T cells and PBMCs.

**Assessment of TCR clonal diversity.** We used NGS to analyze CDR3 in the TCR-β chain and thereby identify unique TCR clones. The unique TCR clones were defined as the TCR clones undetectable in baseline PBMCs but available in the edited T cells of the first cycle. Immunosequencing of the CDR3 of human TCR-β chains was performed using the IR-seq platform from the Geneplus-Beijing Institute[43]. DNA from PBMCs, edited T cells and biopsies was amplified in a bias-controlled multiplex PCR system, followed by high-throughput sequencing. The absolute abundance of each unique TCR-β CDR3 was identified and quantitated. Then, the diversity of the TCR repertoire was calculated based on the Shannon index, similar to that previously described[43].

$$\text{Shannon index} = -\sum_{i=1}^{s} \frac{n_i}{N} \ln \frac{n_i}{N}$$

In this expression, $n_i$ is the clonal size of the T cell clonotype (the number of copies of a specific clonotype), $i$ is the serial number of different clonotypes, $i = 1, \ldots, n$, $S$ is the number of different clonotypes and $N$ is the total number of TCR sequences analyzed.

**Immunohistochemistry staining.** For immunohistochemistry staining, tumors were fixed in 10% phosphate-buffered formaldehyde, embedded in paraffin and sectioned. Formalin-fixed, paraffin-embedded tissues were cut into 4-µm-thick sections and placed on plus-charged slides. Slides were heated at 65 °C overnight, and then were deparaffinized in xylene, hydrated through graded alcohols and water, pretreated by microwaving in Tris-EDTA buffer and treated for endogenous peroxidases with 3% hydrogen peroxide in PBS. Subsequently, immunostaining was performed by incubating with primary antibodies directed against CD3, CD8 or CD68 (PGM-1) (1:100, Dako) overnight at 4 °C. Then, slides were incubated with enzyme-labeled secondary antibody reagent (Dako) for 45 min at room temperature, followed by the ultraView DAB Detection on a Ventana Ultra instrument. Slides were analyzed under an optical microscope (Olympus), and analyzed using ImageJ software (v.1.47).

**Detection of cytokines.** Peripheral blood was collected in red-top tubes (CDRICH, BD Biosciences) and was processed within 2 h in the Department of Laboratory Medicine in the West China Hospital, which is certified by the College of American Pathologists. The serum of peripheral blood was separated and purified for cytokine detection. IL-10 and TNF-α were measured using chemiluminescence (IMMULITE 1000, Siemens). IL-6 was measured using rate nephelometry (IMMAGE800, Beckman Coulter).

**Statistical analysis.** We used the Kaplan–Meier method to summarize time-to-event variables including PFS and overall survival. PFS is defined as time from the date of first edited T cell infusion to the date of disease progression or death due to any reason. Overall survival is the duration from date of first edited T cell infusion to the date of death due to any reason. A subject who had not experienced disease progression before the cut-off date was censored at the last disease assessment date. Subjects alive until the cut-off date were censored at the last time at which they were known to be alive for overall survival analysis. IFN-γ production was compared between pre- and postedited T cells using two-tailed paired *t*-test. TCR diversity was compared between patients and healthy donors with the two-tailed Wilcoxon rank-sum test. Immunohistochemistry staining density was semiquantified by ImageJ software (v.1.47), and then compared using one-way analysis of variance with Sidak's multiple comparisons test. Statistical significance was set at $P \leq 0.05$ (two-sided). All other analyses, including those of AEs, efficacy and immunologic data, were descriptive. All analyses were performed using Prism, v.7.0 (GraphPad) or SPSS, v.22.0.

**Reporting Summary.** Further information on research design is available in the Nature Research Reporting Summary linked to this article.

## Data availability

All requests for raw and analyzed data and materials are promptly reviewed by the West China Hospital to verify whether the request is subject to any intellectual property or confidentiality obligations. Patient-related data not included in the paper were generated as part of clinical trials and may be subject to patient confidentiality. Any data and materials that can be shared will be released via a material transfer agreement. All other data that support the findings of this study will be provided by the corresponding author upon reasonable request when possible. Raw data for Figs. 2–4 and Extended Data Figs. 1–3, 6 and 8–10 are in the Source Data. The raw sequencing data reported in the study have been deposited in the Genome Sequence Archive for Human (http://bigd.big.ac.cn/gsa-human/) at the BIG Data Center, Beijing Institute of Genomics, Chinese Academy of Sciences, under accession number PRJCA002488.

## References

34. Curti, B. D. et al. Phase I trial of anti-CD3-stimulated CD4+ T cells, infusional interleukin-2, and cyclophosphamide in patients with advanced cancer. *J. Clin. Oncol.* **16**, 2752–2760 (1998).
35. Edge, S. B. et al. *AJCC Cancer Staging Manual* 7th edn (Springer, 2010).
36. Li, H. & Durbin, R. Fast and accurate short read alignment with Burrows–Wheeler transform. *Bioinformatics* **25**, 1754–1760 (2009).

37. Tarasov, A., Vilella, A. J., Cuppen, E., Nijman, I. J. & Prins, P. Sambamba: fast processing of NGS alignment formats. *Bioinformatics* **31**, 2032–2034 (2015).
38. Kim, S. et al. Strelka2: fast and accurate calling of germline and somatic variants. *Nat. Methods* **15**, 591–594 (2018).
39. Zhou, H. et al. Whole genome analysis of CRISPR Cas9 sgRNA off-target homologies via an efficient computational algorithm. *BMC Genomics* **18**, 826 (2017).
40. Kim, D. et al. Digenome-seq: genome-wide profiling of CRISPR-Cas9 off-target effects in human cells. *Nat. Methods* **12**, 237–243 (2015).
41. Wang, Z. et al. Application of single-molecule amplification and resequencing technology for broad surveillance of plasma mutations in patients with advanced lung adenocarcinoma. *J. Mol. Diagn.* **19**, 169–181 (2017).
42. Shen, B. et al. Efficient genome modification by CRISPR-Cas9 nickase with minimal off-target effects. *Nat. Methods* **11**, 399–402 (2014).
43. Jia, Q. et al. Local mutational diversity drives intratumoral immune heterogeneity in non-small cell lung cancer. *Nat. Commun.* **9**, 5361 (2018).

## Acknowledgements

This clinical trial was supported by the 1.3.5 Project for Disciplines of Excellence, West China Hospital, Sichuan University (grant no. ZYJC18001); the West China Hospital Foundation of New Technology (grant nos. XJS2016003 and 190160012); the Sichuan Cancer Society Foundation (grant no. SCS-KT001); the National Science and Technology Major Project (grant no. 2017ZX09304023); and the National Natural Science Foundation of China (grant no. 81672982). We thank all of the study participants, H. Wakelee and G. P. Gao for providing insightful advice on this study, J.S. Kim for advice on the off-target effects, J.Y. Li and the nursing team for clinical care, Q. Lu for data collection, Q. Zhang for clinical ECG diagnosis, L. Wang for supporting preclinical study, J. Jiang for data and safety monitoring, M. Zhao for data management and S. Wang for statistical support.

## Author contributions

Y. Lu, J.X., L.D. and T.M. were involved in study design. Y. Lu and T.D. contributed to study concepts. T.D., K.Y. and Y. Zeng were responsible for manufacturing of therapeutic cells. X. Zhou, M.H., R.T., Z.D., Y.G., J.Z., Yongsheng Wang, L.L., Y. Zhang, Y. Liu, B.Z., M.Y., L.Z., Y. Li, Q. Z. and B.Y. were involved in data acquisition. Y. Lu, Yu Wang, H.S. and M.L were involved in quality control of data and algorithms. J.X., X. Zhou, X.Y., J.S., J.L., Yuqi Wang, X.S., W.W., X. Zhang, L.Y., X.X. and C.C. were involved in data analysis and interpretation. Yu Wang and H.S. contributed to statistical analysis. Y. Lu, J.X., R.T. and T.M. wrote the manuscript. Yuquan Wei and W.L. were involved in administrative support and supervision. All authors approved the article for submission and publication.

## Competing interests

The authors declare no competing interests.

## Additional information

**Extended data** is available for this paper at https://doi.org/10.1038/s41591-020-0840-5.

**Supplementary information** is available for this paper at https://doi.org/10.1038/s41591-020-0840-5.

**Correspondence and requests for materials** should be addressed to Y.L.

**Peer review information** Saheli Sadanand was the primary editor on this article and managed its editorial process and peer review in collaboration with the rest of the editorial team.

**Reprints and permissions information** is available at www.nature.com/reprints.

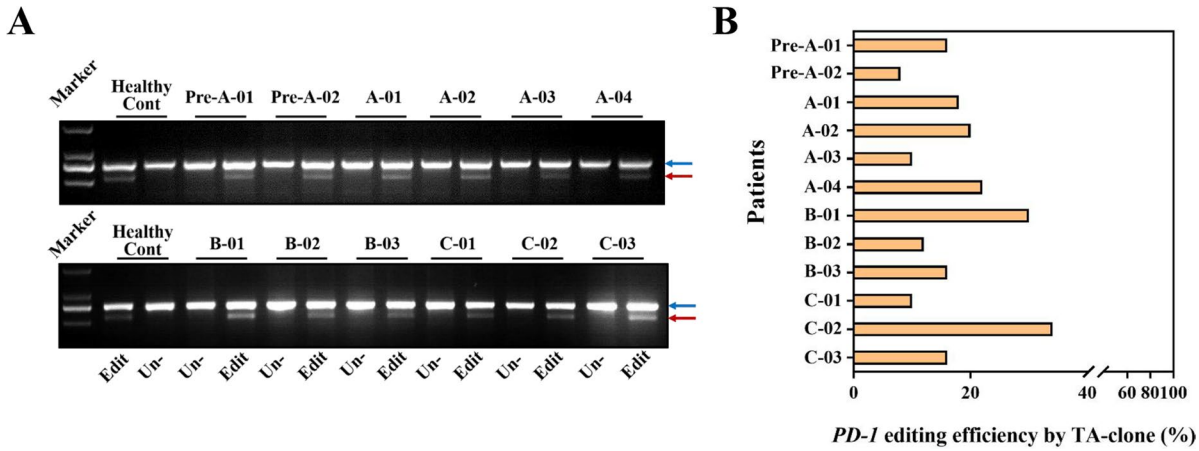


**Extended Data Fig. 1 | T7E1 cleavage assay, TA cloning sequencing of *PD-1* disruption in cultured T cells. a**, DNA amplified from edited or unedited T cells were subjected to T7E1 cleavage assay. T cells from a healthy person served as a control. The blue arrow indicates the expected bands for uncut (no mismatch) *PD-1*; the red arrow, expected bands from the T7E1 assay. Marker, DL2000 Marker (Innova GENE Biosciences, Ontario, Canada). **b**, The efficiency of *PD-1* editing was analyzed by TA cloning on day 21 after electroporation.

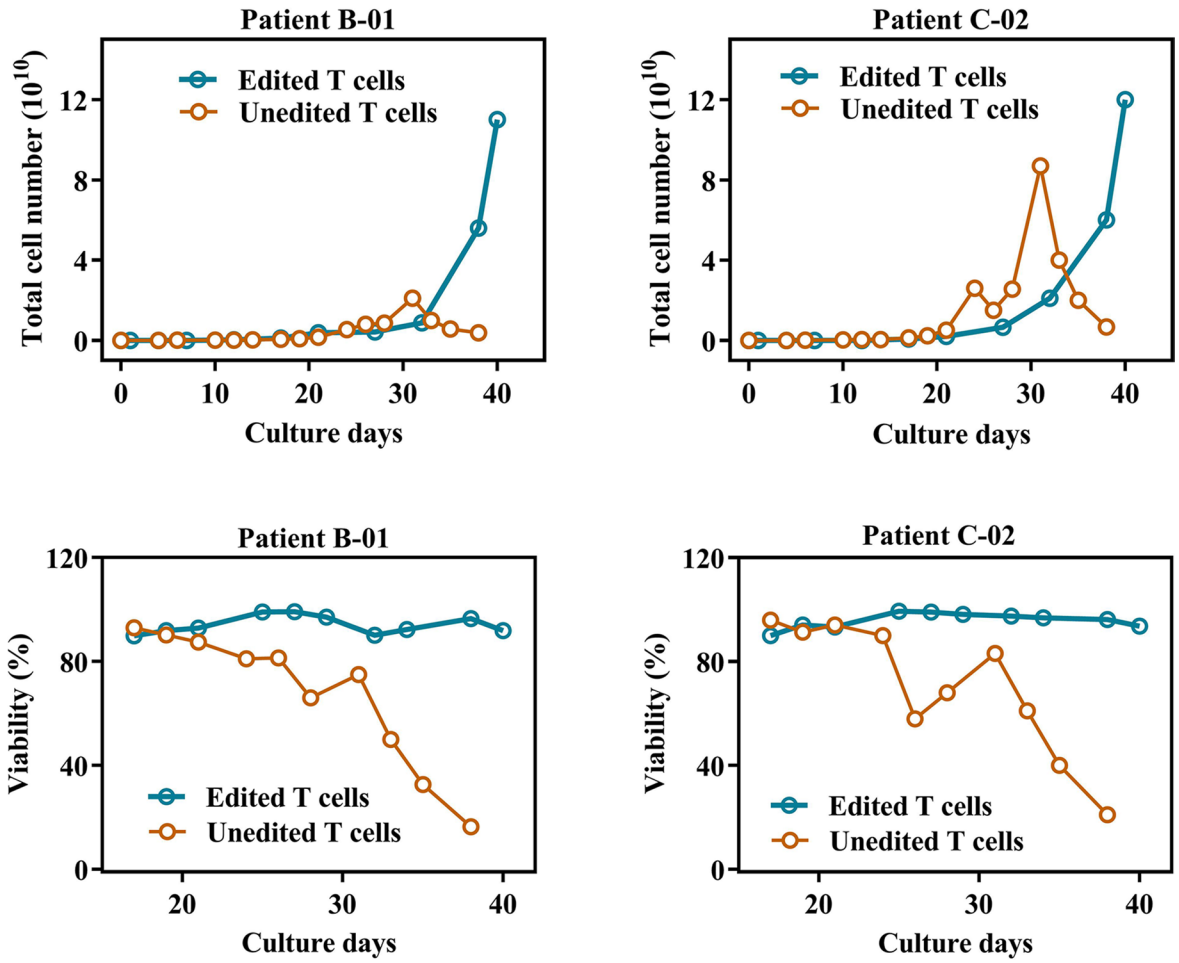


**Extended Data Fig. 2 | Long-term effects of *PD-1* disruption in cultured T cells in Patient B-01 and C-02.** Viability of *PD-1* disruption in long-term cultured T cells. Compared to the rapid decrease in viability of unedited T cells after day 30, the viability of edited T cells was over 90% and remained high until day 40. Total cell numbers of *PD-1* disruption in long-term cultured T cells. The numbers of edited T cells increased slowly until around day 30, reflecting delayed proliferation likely due to the electroporation procedure; after day 30, the numbers of edited T cells increased rapidly. By contrast, the numbers of unedited cells, decreased rapidly after day 30.

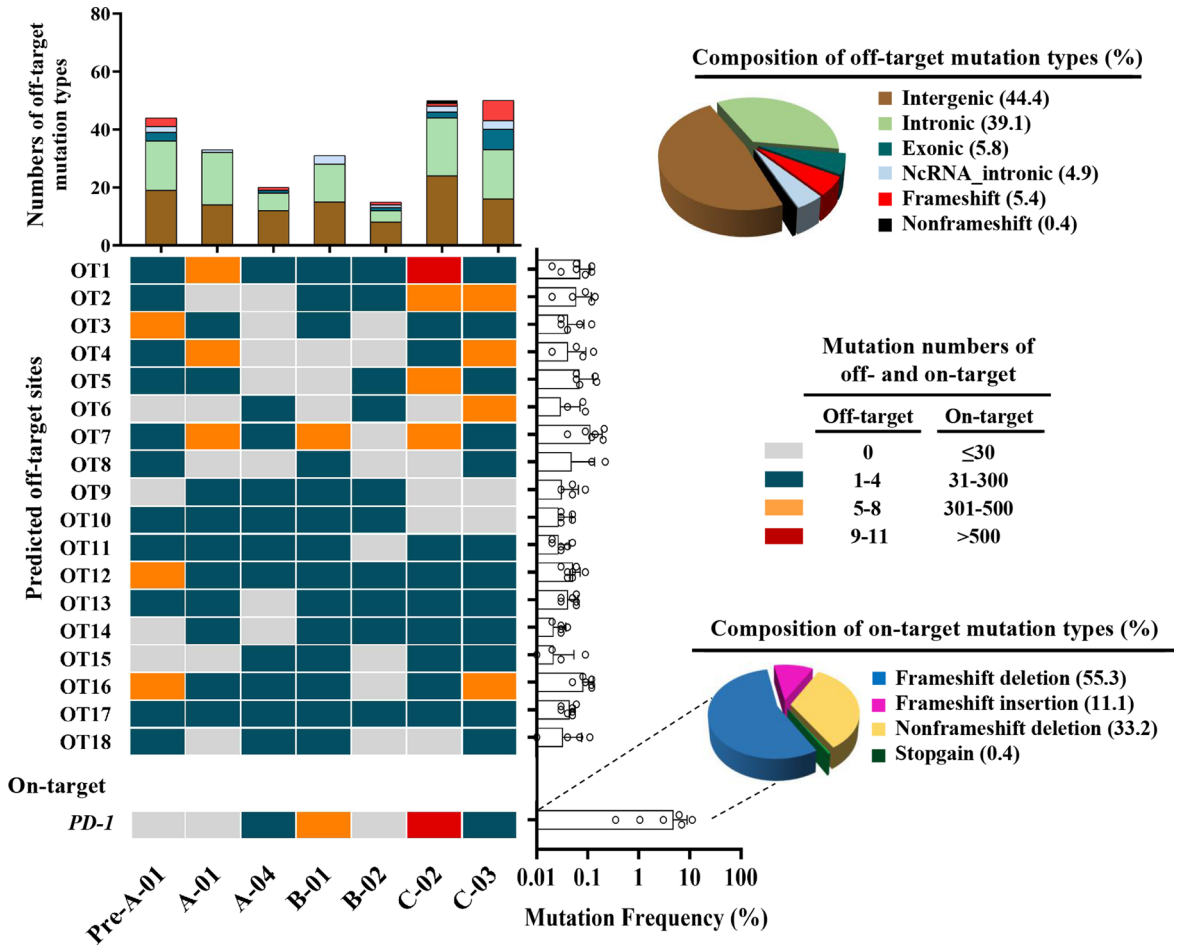


**Extended Data Fig. 3 | Off-target analysis by next generation sequencing (NGS).** Characteristics of on-target and off-target mutation types, frequencies and numbers determined by next-generation sequencing (NGS) for the edited T cells of 7 patients prior to the second cycle of infusion. Bar graph and pie graph above represent the types, the numbers and the composition of off-target mutation, color-coded according to the legend in the top-right corner. Intergenic (44.4%) and intronic (39.1%) mutations composed the majority proportion. Heatmap shows the mutation number of predicted off-target sites (18 off-target sites, OT1-18) and on-target site for individuals. Bar graph on right represents mean mutation frequencies of each site among the 7 patients. The mutation frequencies at these off-target sites and the on-target site were 0.05% (range 0.00–0.22%) and 4.09%, respectively. The modification ratio of on-target/off-target was 105.2. Pie graph on bottom-right shows the composition of on-target mutation. The mutation types of on-target consisted of frameshift or nonframeshift (deletion/insertion mutation), and stopgain, while the vast majority was the deletion mutation (88.5%). Data in bar graph are shown as mean ± s.d.

**A**

Day 1 before infusion

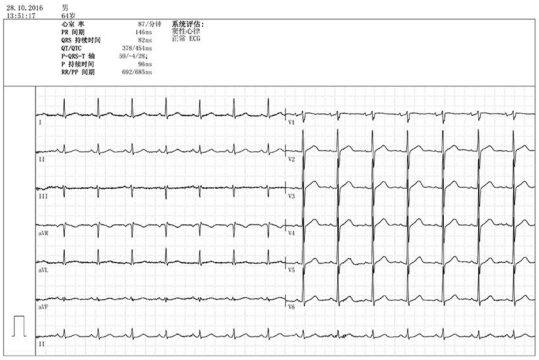

Day 1 after infusion

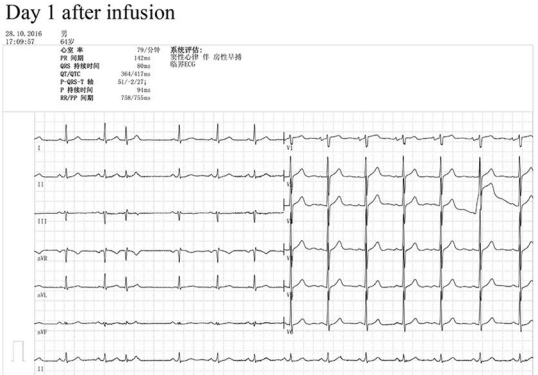

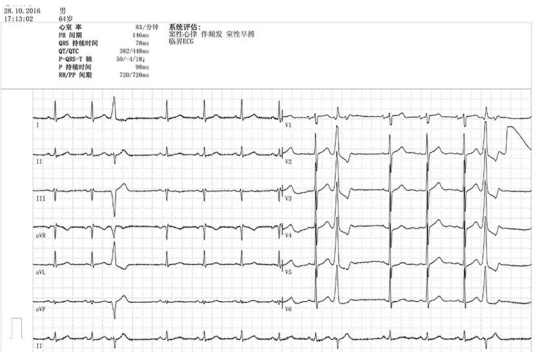

Day 113 after infusion

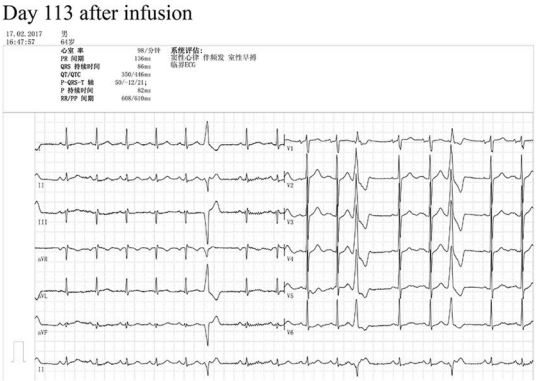

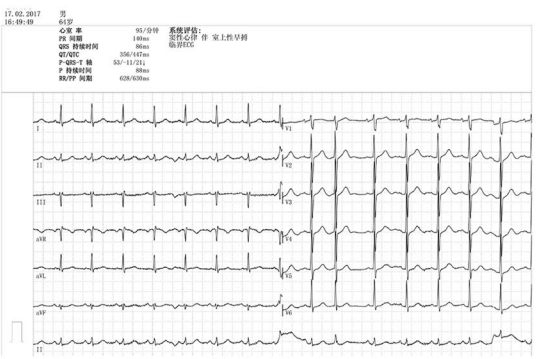

**B**

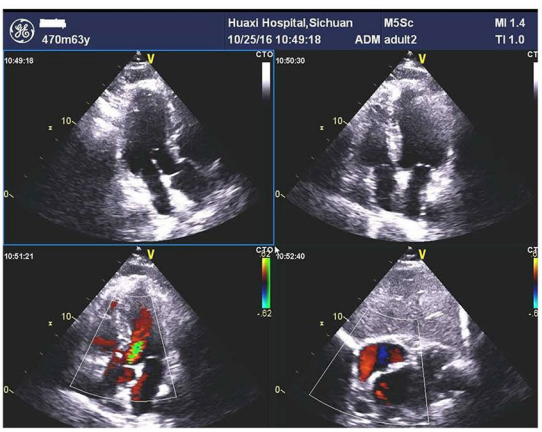


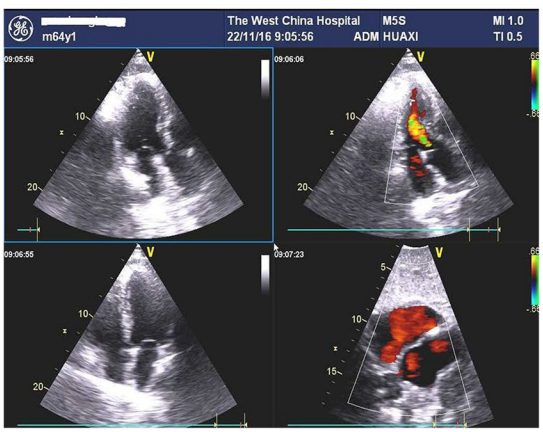


**Extended Data Fig. 4 | See next page for caption.**

**Extended Data Fig. 4 | Electrocardiograph and echocardiography of patient Pre-A-01 during treatment. a**, Electrocardiograph images of patient Pre-A-01 during T-cell therapy. Patient Pre-A-01 had no history of heart disease. The baseline electrocardiograph (before infusion) showed normal results. However, the electrocardiograph on day 1 after the first infusion showed a premature beat; the electrocardiograph on the day 113 showed a premature beat similar to that on day 1. Each image is representative of 3 independent tests. **b**, Representative images from baseline echocardiography (before infusion, left) and echocardiography conducted on day 26 after the first infusion (right). No cardiac lesion or obvious change in functional parameters was found.

| Characteristics | Cohort | | | | |
|---|---|---|---|---|---|
| | Pre-A (n=2) $2\times10^7$/kg | A (n=4) $1\times10^7$/kg | B (n=3) $2\times10^7$/kg | C (n=3) $4\times10^7$/kg | Total (n=12) |
| Age, median (range), years | 55·5 (48–63) | 56 (48–66) | 55 (31–68) | 53 (47–61) | 54·5 (31–68) |
| Sex, n (%) | | | | | |
| Male | 2 (100) | 2 (50) | 1 (33) | 3 (100) | 8 (67) |
| Female | 0 (0) | 2 (50) | 2 (67) | 0 (0) | 4 (33) |
| Smoking status, n (%) | | | | | |
| Never smoker | 0 (0) | 2 (50) | 3 (100) | 0 (0) | 5 (42) |
| Current/former smoker | 2 (100) | 2 (50) | 0 (0) | 3 (100) | 7 (58) |
| ECOG performance status, n (%) | | | | | |
| 0 | 0 (0) | 1 (25) | 0 (0) | 1 (33) | 2 (17) |
| 1 | 2 (100) | 3 (75) | 3 (100) | 2 (67) | 10 (83) |
| Tumor histology, n (%) | | | | | |
| Squamous | 1 (50) | 0 (0) | 1 (33) | 0 (0) | 2 (17) |
| Non-squamous | 1 (50) | 4 (100) | 2 (67) | 3 (100) | 10 (83) |
| CNS metastases, n (%) | 0 (0) | 2 (50) | 1 (33) | 2 (67) | 5 (42) |
| Prior intracranial radiation, n (%) | 0 (0) | 2 (50) | 1 (33) | 1 (33) | 4 (33) |
| Mutational status, n (%) | | | | | |
| EGFR+ | 0 (0) | 1 (25)* | 1 (33)# | 1 (33)& | 3 (25) |
| ALK+ | 0 (0) | 0 (0) | 0 (0) | 0 (0) | 0 (0) |
| PD-L1 expression, n (%) | | | | | |
| <50% | 0 (0) | 2 (50) | 3(100) | 1 (33) | 6 (50) |
| ≥50% | 2 (100) | 2 (50) | 0 (0) | 2 (67) | 6 (50) |

EGFR+, mutation(s) in the EGFR gene.

ALK+, rearrangements in anaplastic lymphoma kinase (ALK).

CNS, central nervous system; ECOG, Eastern Cooperative Oncology Group; PD-L1, programmed death ligand-1;
* EGFR L858R mutation; # EGFR 19 del mutation; & EGFR L861Q mutation

**Extended Data Fig. 5 |** Baseline characteristics of all treated patients.

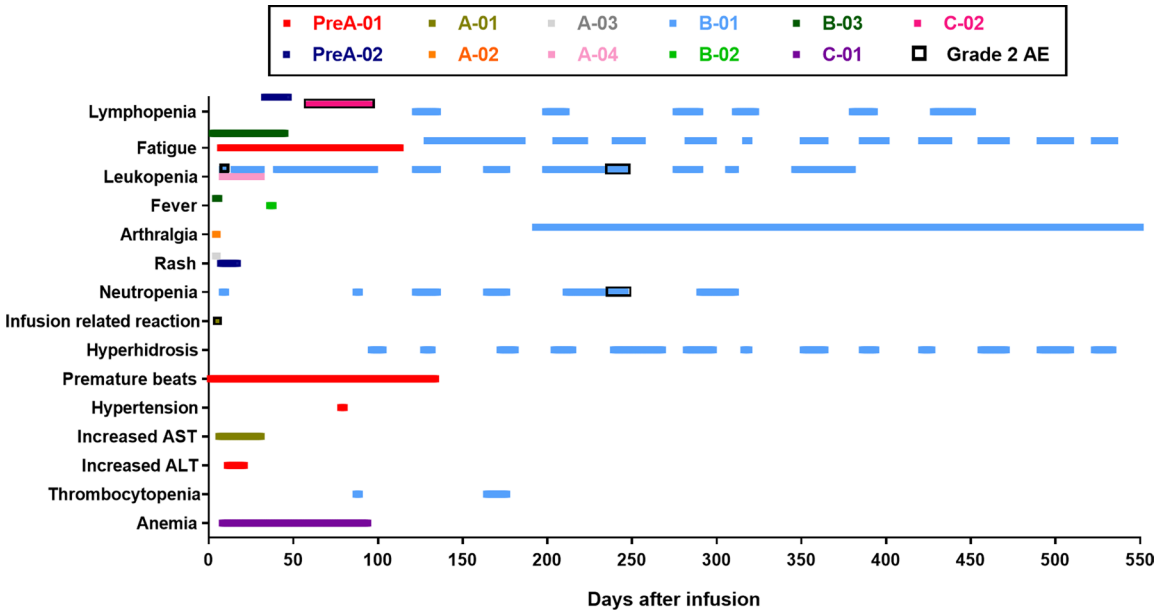


**Extended Data Fig. 6 | Duration of treatment-related adverse events.** Different colors are used to represent each patient. Bar length represents duration of the adverse effect. All related AEs were grade 1 or 2. Grade 2 AEs are outlined in black.

A

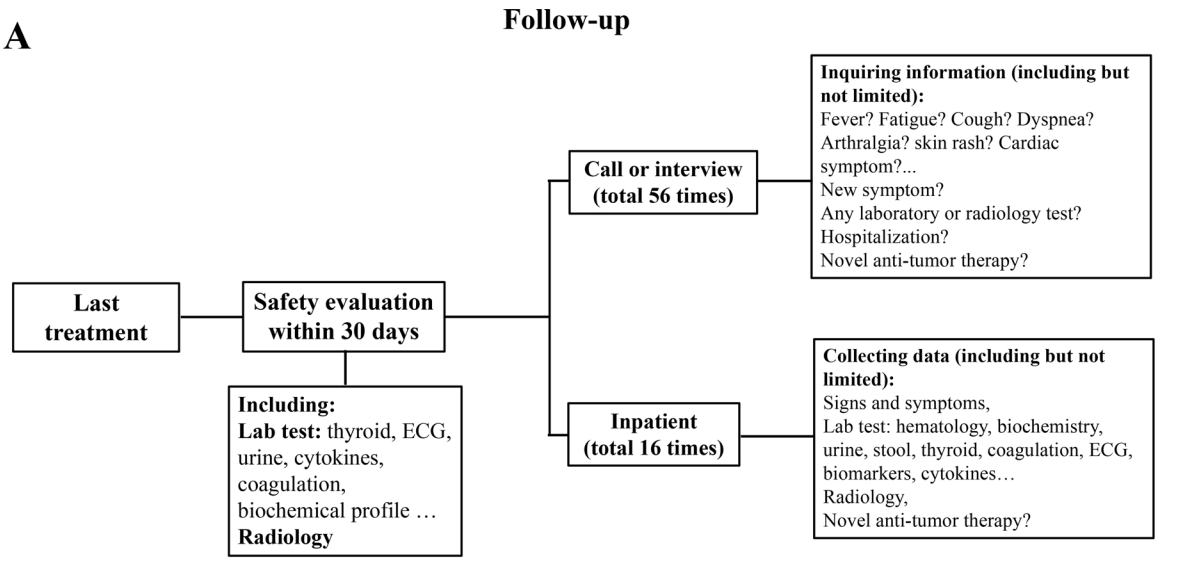


B

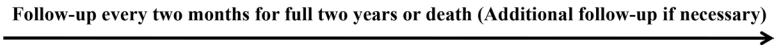


**Summary of treatment-related AEs and SAEs during follow up**

| Events | AE*, Grade (n) | | | SAE, Grade (n) | | | | |
|---|---|---|---|---|---|---|---|---|
| | 1 | 2 | ⩾3 | 1 | 2 | 3 | 4 | 5 |
| Lymphopenia | 1 | 0 | 0 | 0 | 0 | 0 | 0 | 0 |
| Arthralgia | 1 | 0 | 0 | 0 | 0 | 0 | 0 | 0 |
| Anemia | 1 | 0 | 0 | 0 | 0 | 1 | 0 | 0 |
| Herpes zoster | 0 | 0 | 0 | 1 | 0 | 0 | 0 | 0 |
| Lung infection | 0 | 0 | 0 | 0 | 0 | 2 | 0 | 0 |
| Epilepsia | 0 | 0 | 0 | 0 | 0 | 0 | 1 | 0 |

All data presented as n.
Note: Asterisk represents original treatment-related AE. All SAEs were not evaluated as treatment-related. AE, adverse event, SAE, severe adverse event

**Extended Data Fig. 7 | Follow-up diagram and data. a**, Follow-up diagram after treatment. **b**, Summary of treatment-related AEs and severe adverse events (SAEs) during follow-up.

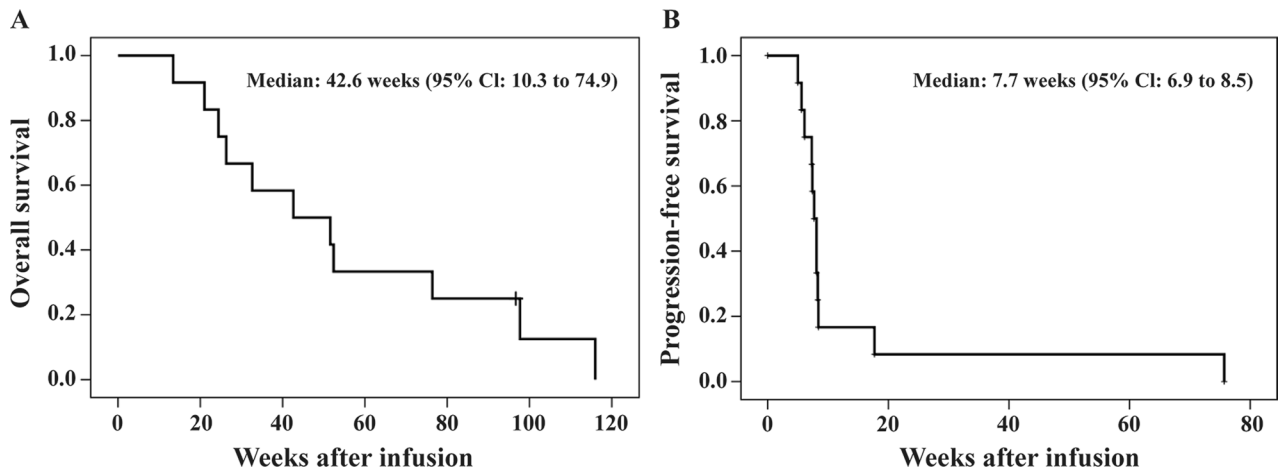


**Extended Data Fig. 8 | Kaplan-Meier estimates of survival in 12 patients.** **a**, Overall survival. **b**, Progression-free survival.

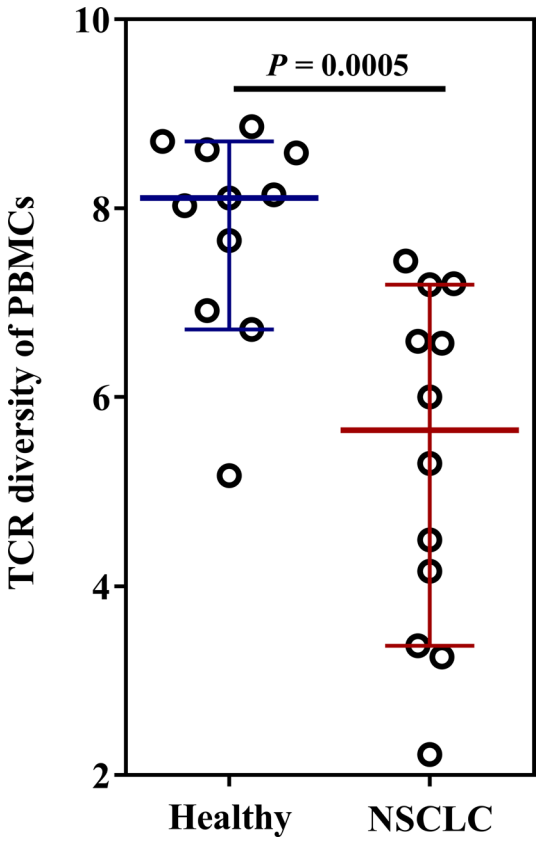


**Extended Data Fig. 9 | TCR diversity in healthy donors and patients.** Comparison of TCR diversity (Shannon index) in PBMCs of 11 healthy donors (n = 11) and 12 patients with refractory NSCLC (n = 12). Data are shown as median ± 95% confidence interval [CI], each dot represents an individual data. *P* value was calculated using the two-tailed Wilcoxon rank-sum test. Median of differences was -2.457, 95% CI for difference was −4.096 to −1.067, *P* = 0.0005.

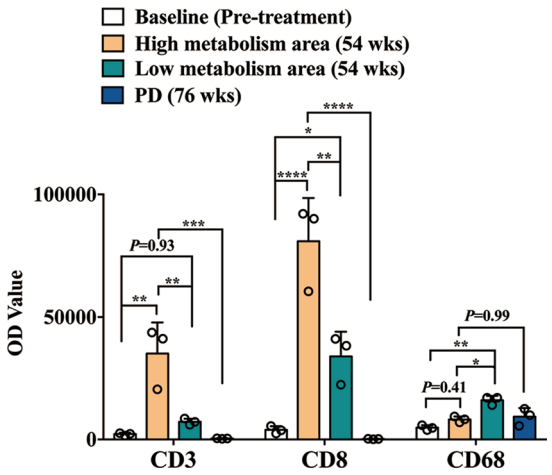


**Extended Data Fig. 10 | The immunohistochemistry staining density was semi-quantified by ImageJ software.** The data was compared using one-way Anova with Sidak's multiple comparisons test (n = 3 per group). Data are shown as mean ± s.d., * $P < 0.05$, ** $P < 0.01$, *** $P < 0.001$ and **** $P < 0.0001$.

nature research

Corresponding author(s): Prof. You Lu, NMED-A99256B

Last updated by author(s): Feb 22, 2020

# Reporting Summary

Nature Research wishes to improve the reproducibility of the work that we publish. This form provides structure for consistency and transparency in reporting. For further information on Nature Research policies, see Authors & Referees and the Editorial Policy Checklist.

## Statistics

For all statistical analyses, confirm that the following items are present in the figure legend, table legend, main text, or Methods section.

| n/a | Confirmed | |
|---|---|---|
| ☐ | ☒ | The exact sample size (*n*) for each experimental group/condition, given as a discrete number and unit of measurement |
| ☐ | ☒ | A statement on whether measurements were taken from distinct samples or whether the same sample was measured repeatedly |
| ☐ | ☒ | The statistical test(s) used AND whether they are one- or two-sided<br>*Only common tests should be described solely by name; describe more complex techniques in the Methods section.* |
| ☒ | ☐ | A description of all covariates tested |
| ☒ | ☐ | A description of any assumptions or corrections, such as tests of normality and adjustment for multiple comparisons |
| ☐ | ☒ | A full description of the statistical parameters including central tendency (e.g. means) or other basic estimates (e.g. regression coefficient) AND variation (e.g. standard deviation) or associated estimates of uncertainty (e.g. confidence intervals) |
| ☐ | ☒ | For null hypothesis testing, the test statistic (e.g. *F*, *t*, *r*) with confidence intervals, effect sizes, degrees of freedom and *P* value noted<br>*Give P values as exact values whenever suitable.* |
| ☒ | ☐ | For Bayesian analysis, information on the choice of priors and Markov chain Monte Carlo settings |
| ☒ | ☐ | For hierarchical and complex designs, identification of the appropriate level for tests and full reporting of outcomes |
| ☒ | ☐ | Estimates of effect sizes (e.g. Cohen's *d*, Pearson's *r*), indicating how they were calculated |

*Our web collection on statistics for biologists contains articles on many of the points above.*

## Software and code

Policy information about availability of computer code

| | |
|---|---|
| Data collection | Electronic Case Report Forms (eCRF) (version: 3.0) for clinical data. Nucleofector 2b device (Lonza, Germany) for preparation of edited T cells, Veriti thermocycler (Applied Biosystems, USA) for T7E1 cleavage assay, FACSAria II flow cytometry (BD Biosciences, CA), Ventana Ultra instrument (USA) and optical microscope (Olympus, Leica S3, Japan) for immunohistochemistry staining, IMMAGE 800 (Beckman Coulter, USA) for IL-6 data, IMMULITE 1000 (Siemens, UK) for IL-8 and TNF-a data,, Illumina (San Diego, CA), HiSeq X Ten instrument (Illumina, USA) and MiSeq Reporter (Illumina, USA) for tracking of edited cells; NovaSeq 6000 platform (Illumina) for WGS data, Fastq join (version 1.3.1) program for NGS data; sgRNAcas9 software (version 2.0.6) for predicting off-targets by NGS; Cas-OFFinder (version 2.4) for predicting potential off-target sites by WGS. |
| Data analysis | MedDRA (version 21.0) for AE analysis; Paired Student's t test for IFN-γ production analysis; The exact Wilcoxon test for TCR diversity analysis; ImageJ software (version 1.47) for immunohistochemistry staining density; samtools (version1.1), sambamba (version 0.6.8), strelka2 (version 125 2.8.3), Fusionmap (version 10.0.1.29) and ANNOVAR (version 2019Oct24) for WGS data analysis; SPSS 22.0 for OS and PFS data analysis; FlowJo software (version 7.6.1) for flow cytometry analysis; Details of the all data analysis are included in the Methods. |

For manuscripts utilizing custom algorithms or software that are central to the research but not yet described in published literature, software must be made available to editors/reviewers. We strongly encourage code deposition in a community repository (e.g. GitHub). See the Nature Research guidelines for submitting code & software for further information.

## Data

Policy information about availability of data

All manuscripts must include a data availability statement. This statement should provide the following information, where applicable:

- Accession codes, unique identifiers, or web links for publicly available datasets
- A list of figures that have associated raw data
- A description of any restrictions on data availability

The data that support the findings of this study will be provided by corresponding authors upon reasonable request.

# Field-specific reporting

Please select the one below that is the best fit for your research. If you are not sure, read the appropriate sections before making your selection.

☒ Life sciences ☐ Behavioural & social sciences ☐ Ecological, evolutionary & environmental sciences

For a reference copy of the document with all sections, see nature.com/documents/nr-reporting-summary-flat.pdf

# Life sciences study design

All studies must disclose on these points even when the disclosure is negative.

| | |
|---|---|
| Sample size | This is a standard 3+3 designed for phase I dose-escalation trial. And added a cohort Pre-A aims to assure the safety of trial. So size of enrolled 10 patients were designed in four cohorts (cohort Pre-A, A, B and C). During the trial, cohort Pre-A added one patient for consideration of safety because of the first patient (Pre-A-01) suffering from arrhythmia. Cohort A added one patient (A-04) due to patient (A-03) early withdrawal from trial. Finally, the actual sample size was 12 patients for evaluation of safety and feasibility in this trial. |
| Data exclusions | No data was excluded from the analysis. |
| Replication | We included data on all available patients/samples in all figures. |
| Randomization | There was no randomization in this phase I single arm study. |
| Blinding | There was no blinding as the paper reports a phase I single arm study. |

# Reporting for specific materials, systems and methods

We require information from authors about some types of materials, experimental systems and methods used in many studies. Here, indicate whether each material, system or method listed is relevant to your study. If you are not sure if a list item applies to your research, read the appropriate section before selecting a response.

### Materials & experimental systems

| n/a | Involved in the study |
|---|---|
| ☐ | ☒ Antibodies |
| ☒ | ☐ Eukaryotic cell lines |
| ☒ | ☐ Palaeontology |
| ☒ | ☐ Animals and other organisms |
| ☐ | ☒ Human research participants |
| ☐ | ☒ Clinical data |

### Methods

| n/a | Involved in the study |
|---|---|
| ☒ | ☐ ChIP-seq |
| ☐ | ☒ Flow cytometry |
| ☒ | ☐ MRI-based neuroimaging |

## Antibodies

Antibodies used

1. Antibodies used for flow cytometry
Antigen, Antibody Clone, Manufacturer, Catalog number, Working dilution, Lot number
CD3-BV510, HIT3a, BD Biosciences, 564713, 1:50, 9164820
CD4-BV421, RPA-T4, BD Biosciences, 562424, 1:50, 8187880
CD8-PE, HIT8a, BD Biosciences, 555635, 1:50, 8299501
PD-1-APC, MIH4, BD Biosciences, 558694, 1:50, 7075610
IFN-γ-PE, B27, BD Biosciences, 554701, 1:50, 8354864
CD8-APC-Cy7, BD Biosciences, 557834, 1:50, 8184768
2. Antibodies used for immunohistochemstry
Antigen, Antibody Clone, Manufacturer, Catalog number, working dilution, lot number.
PD-L1, Ventana SP142, Roche, 740-4859, neat, E29397
secondary antibody: DAB, Roche, 760-500, neat, F13568

CD3, LN10, ZSGB-BIO, ZM0417, 1:100, 2005005
secondary antibody: DAB, Roche, 760-700, neat, F11441
CD8, C8/144B, DAKO, m7103, 1:100, 20042547
secondary antibody: DAB, Roche, 760-500, neat, F13568
CD68, PGM-1, DAKO, m0876, 1:100, 20036057
secondary antibody: DAB, Roche, 760-500, neat, F13568
3. Antibodies used for T cell expansion and activation
Antibody, Manufacturer, Catalog number, Working dilution, Lot number.
anti-CD3 antibody, OKT3, Novoprotein Scientific Inc, GMP-A018, 1:100, 0331305
anti-CD28 antibody, Novoprotein Scientific Inc, GMP-A063, 1:100, 0331306
IFN-γ Novoprotein Scientific Inc, GMP-CI57, 1:1000, 0331197
IL-2 Beijing Shuanglu Pharmaceutical Co., Ltd., Sinopharm Standard S19991010, 1:1000, 20160308

Validation

All antibodies used in this study are commercially available. Antibodies used in a specific species or application have been appropriately validated by manufacturers for that application and this information is provided on their website and product information datasheets. All antibodies described here have been further optimized for an appropriate concentration by testing several dilutions.

## Human research participants

Policy information about studies involving human research participants

| | |
|---|---|
| Population characteristics | Twelve patients received the planned PD-1 gene edited T-cell therapy are eligible for analysis, the population characteristics of them were provided in Table 1. The median age of the patients was 54.5 (range: 31-68). Four patients were female and 8 were male. Nine patients had 3 previous systemic treatment regimens. Three patients had more than 3 previous systemic treatment regimens. Two patients were previously treated with PD1 antibody. |
| Recruitment | Patients were recruited through recruitment advertisement which was approved by the Institutional Review Board of West China Hospital, Sichuan University. The recruitment advertisement was put up as a poster in bulletin board of GCP, West China Hospital. Patients were enrolled on a first-come-first-served basis. There was no potential self-selection bias in recruiting patients. Twenty-two patients were enrolled based upon the inclusion and exclusion criteria in this phase I clinical trial. All patients were explained and written and signed informed consent was obtained prior to enrollment. |
| Ethics oversight | The study protocol and subsequent amendments (Necessary additional data) were approved by the Institutional Review Board of West China Hospital, Sichuan University, Chengdu, China (2016 Review, No. 123). |

Note that full information on the approval of the study protocol must also be provided in the manuscript.

## Clinical data

Policy information about clinical studies

All manuscripts should comply with the ICMJE guidelines for publication of clinical research and a completed CONSORT checklist must be included with all submissions.

| | |
|---|---|
| Clinical trial registration | MHC-001 ClinicalTrials.gov number, NCT02793856 |
| Study protocol | The full trial protocol are available in the supplementary materials for this article. |
| Data collection | For study using Electronic Data Capture (EDC), Version 3.61.3 PROD XKL 20180710 (https://edc.edetek.cn:8443/MHC001/index.action), the designated investigator staff will enter the data required by the protocol into the Electronic Case Report Forms (eCRF). The principal investigator is responsible for assuring that the data entered into eCRF is complete, accurate, and that entry and updates are performed in a timely manner. All data collected at between Aug 26, 2016 and Jan 31, 2020. |
| Outcomes | The primary endpoints of this phase 1 dose escalation study was safety and feasibility. Secondary endpoint was efficacy. Exploration objectives included assessments of T-cell receptor (TCR) clones and in vivo tracking of edited T cells. |

## Flow Cytometry

### Plots

Confirm that:

☒ The axis labels state the marker and fluorochrome used (e.g. CD4-FITC).

☒ The axis scales are clearly visible. Include numbers along axes only for bottom left plot of group (a 'group' is an analysis of identical markers).

☒ All plots are contour plots with outliers or pseudocolor plots.

☒ A numerical value for number of cells or percentage (with statistics) is provided.

### Methodology

| | |
|---|---|
| Sample preparation | Human blood was collected in Red-top tubes (CDRICH®, BD Biosciences) and was processing in research lab. The PD-1 edited T cells were prepared by. MedGenCell, Co., Ltd (Chengdu, China). |

| | |
|---|---|
| Instrument | FACSAria II flow cytometry (BD Biosciences, CA) |
| Software | FlowJo software (version 7.6.1) |
| Cell population abundance | N/A |
| Gating strategy | FSC-A/FSC-H plots were used to determine singlet gates. FSC-A/SSC-A plots were used to determine cell population gates.Isotype controls were used to indicate the boundaries between positive and negative populations. |

☒ Tick this box to confirm that a figure exemplifying the gating strategy is provided in the Supplementary Information.